



ANALYSIS OF AAC BLOCK FOR REDUCING CARBON FOOTPRINT IN MODERN CONSTRUCTION INDUSTRY

Prince Pal
(2000511627014)

Under the Supervision of
Prof. Sawan Kumar Sharma
&
Prof. Shakshi Jain

TO THE

FACULTY OF ARCHITECTURE AND PLANNING
Dr. A.P.J. ABDUL KALAM TECHNICAL UNIVERSITY
LUCKNOW

(Formerly Uttar Pradesh Technical University, Lucknow)

Session 2022-23

CHAPTER 1

INTRODUCTION

1.1 BACKGROUND

As increasing demand for housing and buildings all over the world has resulted in consumption of significant amounts of natural resources in the form of building materials. The traditional bricks are the main building materials that are used extensively in the construction and building industry. The realization of reasons for this has created a shift towards development of sustainable building materials which need less energy in manufacturing and also in the operational cycle of the building.

Autoclaved Aerated Concrete blocks are recently one of the newly adopted building materials. The Autoclaved aerated concrete (AAC) is a product of fly ash which is mixed with lime, cement, and water and an aerating agent. The AAC is mainly produced as cuboid blocks and prefabricated panels. The Autoclaved aerated concrete is a type of concrete that is manufactured to contain lots of closed air voids. The AAC blocks are energy efficient, durable, less dense, and light weight. (Jayasinghe, (2009))



Figure 1



Figure 2

1. Fired bricks are used for construction purposes over thousand years.
2. The traditional brick-making process involves removal of agriculturally productive topsoil rich in clay and soil organic matter contents.
3. Also it involves the process of digging of land for soil, and removal of plants and set up of many smoke chimneys.

➤ **The brick industry has a devastating environmental impact:**

1. They are major contributors to climate change and a significant source of CO₂ emissions, greenhouse gas (GHG) emissions and short-lived climate pollutants (SLCP's).
2. It release over 1,072 million tones of carbon dioxide emissions into the atmosphere every year which is 2.7% of total emissions.
3. Hazardous working conditions.
4. Scavenged, highly polluting fuels are also used these include tyres, wood, waste oil, cow dung, paper, liquid tar (mazoot) and battery casings.
5. Emission black carbon from thousands of kilns directly contributes to glacial melting in the Himalayas and affects monsoonal rainfall patterns.
6. Damage to biodiversity

1.2 AIM

Assessing AAC block as an alternative construction material for wall.

1.3 OBJECTIVES

1. To compare the strength and energy of Autoclaved Aerated concrete block with that of commonly used burnt clay bricks.
2. To assess the embodied energy and contribution to the operational energy of AAC block.
3. To outline the applications of AAC block in various projects.

1.4 METHODOLOGY

1. Studying the concept of AAC block and its efficiencies.
2. Analysing different case studies from various countries that have implemented AAC block as their construction materials.

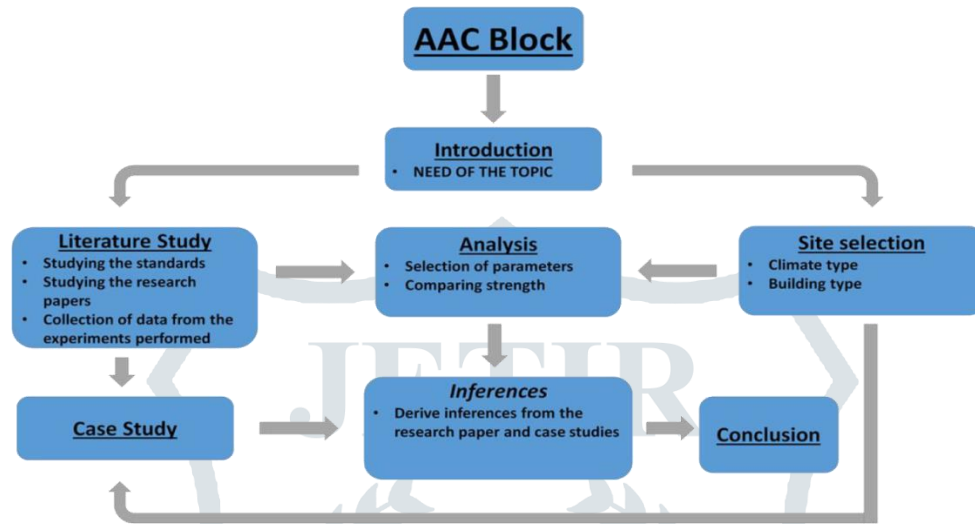


Figure 3 Methodology flowchart

1.5 SCOPE AND LIMITATIONS

1. The dissertation is based on literature study carried out by available sources that include research papers, books and online websites.
2. The study majorly focuses on use of AAC block for wall and the cases based in similar climate

CHAPTER 2

LITERATURE REVIEW

2.1 DEFINITION OF SUSTAINABILITY AND SUSTAINABLE MATERIALS

- 1.Sustainability is the balance between the environment, equity, and economy.
- 2.The integration of environmental health, social equity and economic vitality in order to create thriving, healthy, diverse and resilient communities for this generation and generations to come.



Figure 4-Approach to sustainability

- 3.Sustainable building materials are related to the following criteria:

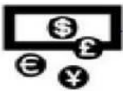


 <div>Transports Development Resources Build ability Fees Lifecycle Balance Popular</div>	 <div>Community Human needs Social equity Meetings Sharing Discovering Cultures Collective</div>	 <div>Ecology Recycling Natural and local materials Renewable materials Climate Health impact</div>
--	---	--

Figure 5-Different sectors for sustainability

- 4.Resource efficiency.
- 5.Pollution prevention (including indoor air quality).
- 6.Energy efficiency (including initial and recurrent embodied energy, and GHG emissions).

2.2 MANUFACTURING PROCESS

Autoclave aerated concrete blocks are also known as Auto claved light weight concrete(ALC) Autoclaved Aerated Concrete (AAC) is one of the eco – friendly and certified green building materials .AAC was perfected in the mid of 1920s by the Swedish architect. It has become one of the most used building materials in Europe and is rapidly growing in many other countries around the world .Basically, AAC is a mixture of cement ,fly ash , sand , water, and aluminum powder. When the materials are proportionally weighed. AAC is using no aggregate larger than sand. Here, Aluminum powder reacts with calcium hydroxide and water to form H_2 .The hydrogen gas foams and doubles the volume of the raw mix creating gas bubbles shown in (figure 1) At the end of the foaming process, the hydrogen escapes into the atmosphere and is replaced by air. When the air are removed from the material, it is solid but still soft. It is then cut into blocks and placed in an cylindrical chamber for 11-.12 hours. (Wahane, 2017)

2.2.1 MATERIAL USED

- **Cement**

Cement is a binder, a substance used in construction industry that sets and hardens and can bind other materials together. The properties of OPC used in the AAC block are



Figure 6

- Color - White
- Density of cement -1440kg/m³
- Type – OPC Grade 53
- Compressive strength – 53 MPa

Compound	Chemical composition (in%)
Cao	57.84
Sio ₂	20.33
Fe ₂ O ₃	4.68
Al ₂ O ₃	3.40
Mgo	1.51
MnO	0.10
TiO ₂	0.09
K ₂ O	0.72
Na ₂ O	0.51
SO ₃	7.26
Loss of ignition	3.42
Insoluble residue	1.23

- Codal provision – IS 269:1989 and IS 383:1970
- Chemical composition of cement (Wahane, 2017)

● Fly ash

Fly ash is waste industrial product used for reduction of construction cost. The density of fly ash ranges from 400-1800kg/m³.



It provides thermal insulation, fire resistance and sound absorption. The type of fly ash used is of Class C with contains 20% lime (CaO) and loss of ignition not be more than 6% (Wahane, 2017)

● Sand

Fine aggregate are basically sand consists of crushed stone with maximum particles passing through a 4.75mm sieve,



As per codal provision IS 383:1970, the silica content shall not be less than 80%. (Wahane, 2017)

- **Lime stone**

Limestone is made up of calcite aragonite. Limestone is obtained either by



crushing to fine powder at AAC factory or by directly purchasing it in powder form from a merchant. (Wahane, 2017)

- **Aluminium powder**

Aluminum is an expansion agent. When the raw material reacts with aluminum powder, air bubble introduced due to reaction between calcium hydroxide, aluminum and water and hydrogen gas is released

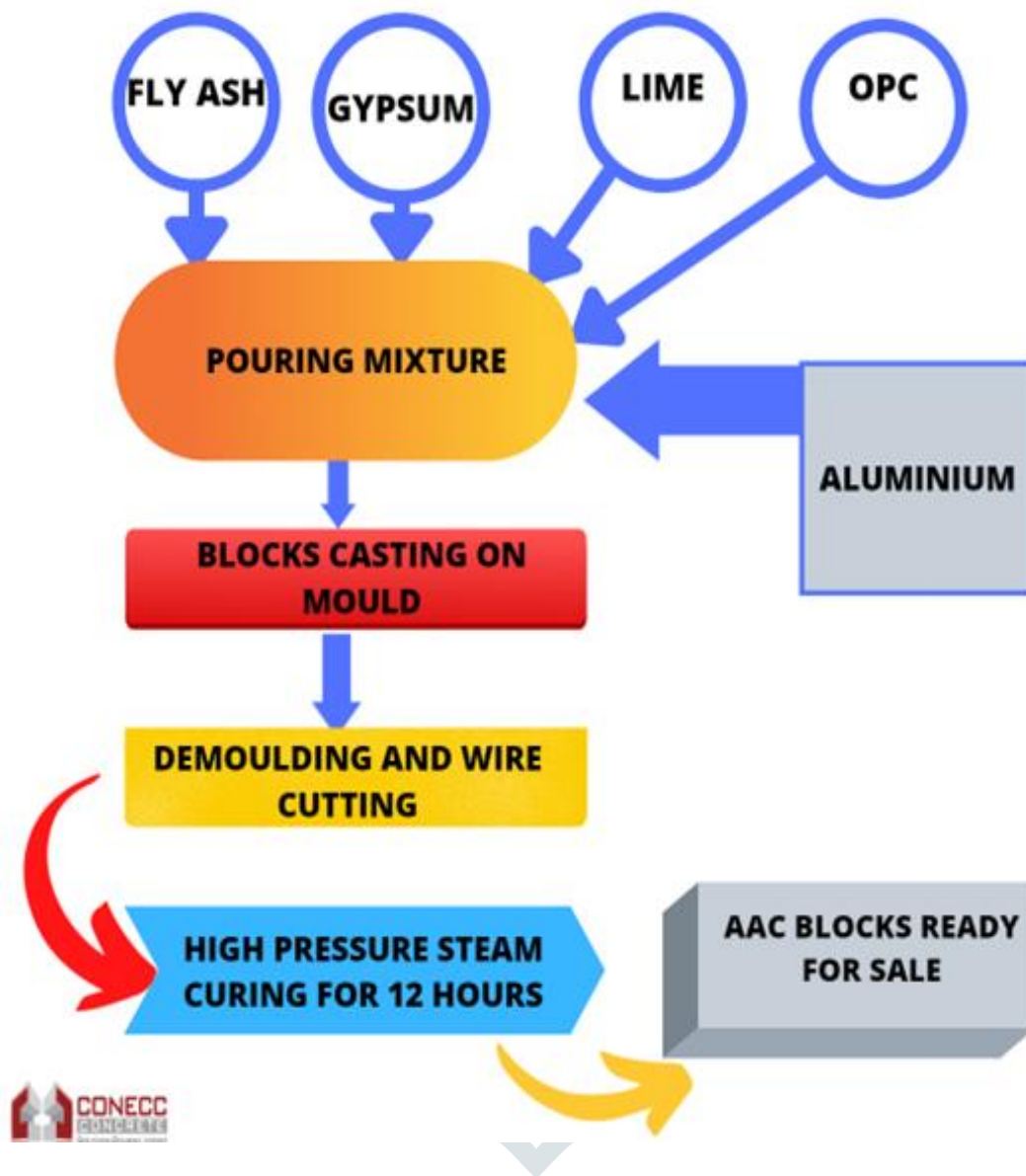


$2\text{Al} + 3\text{Ca}(\text{OH})_2 + 6\text{H}_2\text{O} \rightarrow 3\text{CaO} \cdot \text{Al}_2\text{O}_3 \cdot 6\text{H}_2\text{O} + 3\text{H}_2$ (Wahane, 2017)

- **Gypsum**

Gypsum is easily available in the market and is used in powder form (Wahane, 2017)

2.2.2 FLOWCHART OF MANUFACTURING AAC BLOCK



Stage – 1 Raw Material Preparation

AAC blocks manufacturing process starts with raw material preparation. List of raw materials and relevant details are mentioned below (Wahane, 2017)

➤ Cement

53-grade Ordinary Portland Cement (OPC) from r manufacturer is required for manufacturing AAC blocks. Cement supplied by plants is not recommended due to variations in quality over different batches of cement. (Wahane, 2017)

➤ **Fly ash or sand**

Fly ash is mixed with water to form fly ash slurry. Slurry thus formed is mixed with other ingredients like lime powder, cement, gypsum and aluminium powder in proportionate quality to form blocks (Wahane, 2017)

➤ **Limestone powder**

Lime powder required for AAC production is acquired by crushing limestone to fine powder at AAC factory or by directly purchasing it in powder form from a various plants. (Wahane, 2017)

➤ **Gypsum**

Gypsum is readily available in the market. (Wahane, 2017)

Stage- 2 Dosing and Mixing

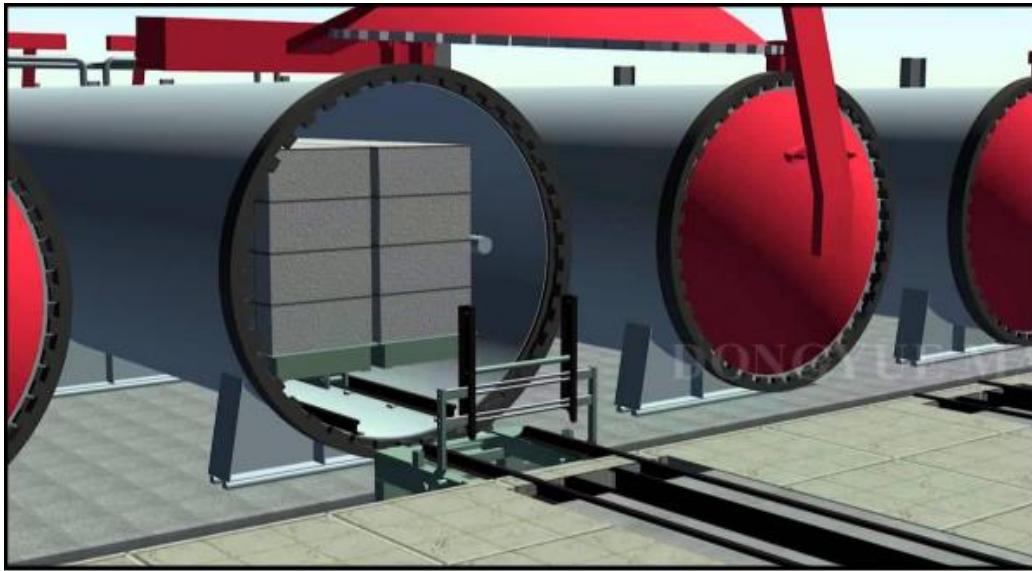
After raw material preparation, next step of AAC blocks manufacturing process is dosing and mixing. Process of dosing and mixing means the quality of final products. Maintaining ratio of all ingredients as –

- FLY ASH OR SAND : LIME : CEMENT : GYPSUM = 69:20:8:3
- Aluminium is about 0.08% of total dry materials in the mix
- Water ratio = 0.60 - 0.65

The cycle of mixing and pouring is 5.5 minutes. A dosing and mixing unit is used to form the correct mix to produce AAC blocks. Fly ash is pumped into a container. Once the desired weight is poured in, pumping is stopped. Similarly lime powder, cement and gypsum are poured into individual containers using conveyors. Once required amount of each ingredient is filled into their individual containers control system releases all ingredients into mixing drum. A smaller bowl type structure used for feeding Aluminium powder is also attached as a part of mixing unit. Once the mixture has been churned for set time, it is ready to be poured into molds using dosing unit. Dosing unit releases this mixture as per set quantities into molds. Dosing and mixing process is carried out continuously because if there is a gap between charging and discharging of ingredients, residual mixture might start hardening and choke up the entire unit. For AAC blocks manufacturing, entire dosing and mixing operation is completely automated and requires minimum human intervention (Wahane, 2017)

Stage- 3 Casting, Rising and Curing

Once mix of raw materials is ready, it poured is in molds. Molds can be of various sizes depending upon installed capacity like 4.2m x 1.2m x 0.65m in size Before casting, molds are coated with a thin layer of oil in order to ensure that green-cake does not stick to molds. While slurry is mixed and poured into greased molds, Aluminum reacts with Calcium Hydroxide and water and releases hydrogen gas. This leads to formation of tiny cells causing slurry mix to expand. Such expansion may be thrice its original volume. Bubble size is about 2-5mm. Thus, this is the reason behind light weight and insulating properties of AAC block. When rising process is over, green-cake is allowed to settle & cure. (Wahane, 2017)



Usually rising and pre-curing process takes around 60-240 minutes. Rising is dependent on raw material mix and weather conditions. Due to this, pre-curing is also referred as ‘heating room pre-curing’. At end of precuring process, green-cake is hard enough to be wire cut as per requirements. Autoclave Aerated concrete is cured in an autoclave – a large pressure vessel. Autoclave is normally a steel tube of 3m diameter and 45 meters long. Steam is fed into the autoclave at high pressure, typically reaching a pressure of 800kPa to 1200 KPa and a temperature of 180°C. (Wahane, 2017)

Stage- 4 Demoulding and Cutting

Once green cake has achieved cutting strength, it is ready to be demoulded and cut as per requirements. Once a mold is out of pre-curing room, it is lifted by a crane for demoulding operation. While all previous processes like raw material preparation, dosing & mixing and casting are pretty much same across all technologies, demoulding and cutting process vary vastly depending on technology provider. Differences in



demoulding and cutting process are also evident from different types of molds required by different technology provider. Primarily cutting process may be classified as flat-cake and tilt-cake based on how green cake is demoulded and sent to cutting line. (Wahane, 2017)

Stage- 5 Autoclaving of AAC blocks

The final process of manufacturing is autoclaving. The wire cut blocks are transported to an autoclaved chamber where is heated to the required temperature. This process gives the desired durability and structural

stability to AAC blocks. The baking is done for about 8-12 hours at a temperature of around 180 degrees. (Wahane, 2017)



The temperature and period of heating determine the grade of the materials. Curing in an autoclave reduces drying shrinkage. The autoclave curing process requires more energy and a more expensive kiln, but it can produce blocks in less time (Wahane, 2017)

The blocks are stacked on pellets on completion of autoclaving process for transporting to the required destinations. All quality tests are conducted in the factory itself. (Wahane, 2017)

2.3 Performance of AAC block under varying temperatures

Autoclaved aerated concrete (AAC) blocks due to their light weight, low density are extensively used as masonry units in construction in spite of these properties there exists a problem of cracking in the AAC units under high temperatures, It is also said that the blocks undergo thermal expansion. The plaster does not get adhered to the surface of units. An effort has been made to determine the strength behaviour, bond behaviour, crack behaviour and thermal behaviour of AAC blocks under varying temperatures, mortar ratios and thickness. It is found that there was reduction in the strength and formation of cracks for temperatures above 500 deg.C, the bond behaviour was found vary with mortar thickness and ratios. Thermal comfort study showed better thermal comfort in comparison with the model with Solid Concrete Block. (Vengalais, ShivakumarMangloor, & Talla Krishna Chaitanya Goud, 2009)

2.3.1 EXPERIMENTAL PROGRAMME

The following materials were used for this study:

➤ AAC BLOCKS

Blocks manufactured using fine aggregates, fly ash by passing hydrogen gas where used for various tests. These AAC blocks of size 600mm×200mm×150mm. (Wahane, 2017) (Vengalais, ShivakumarMangloor, & Talla Krishna Chaitanya Goud, 2009)

➤ Ready JOINT MORTAR

Joint mortar proves to be good in bonding action when used with AAC blocks.

➤ MORTAR-READY PLAST

Plaster mortar proves to be good bonding and acts as an ideal plaster mortar when used with AAC blocks.

Following methodology was adopted to assess the performance of AAC blocks. In this regard a test program was planned and designed to carry out various studies based on the actual site conditions.

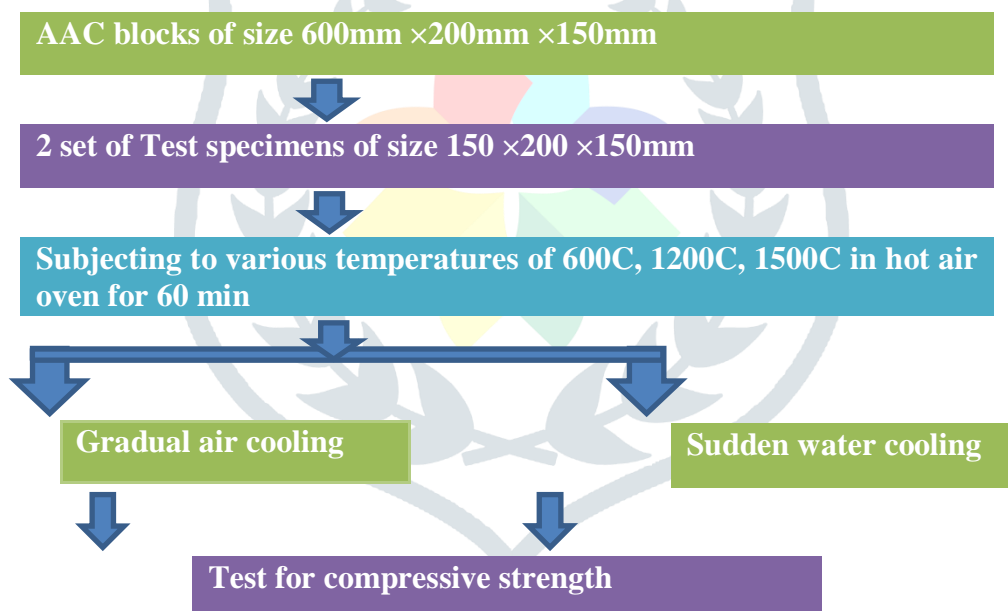
1. Strength behaviour of block specimens under varying temperatures
2. Bond behaviour of masonry joints with varying mortar ratios and thickness.
3. Crack behaviour of prisms made with block specimens under varying temperature.
4. Thermal comfort studies of the AAC blocks in comparison with solid concrete blocks.

Following tests were conducted based on the above mentioned cases

- Compressive strength test
- Behaviour of bond with varying mortar types and thickness
- Crack visibility study
- Thermal comfort study

A. Strength behavior of block specimens under varying temperatures

Gives the flow chart for the strength behaviour of block specimens under varying temperatures



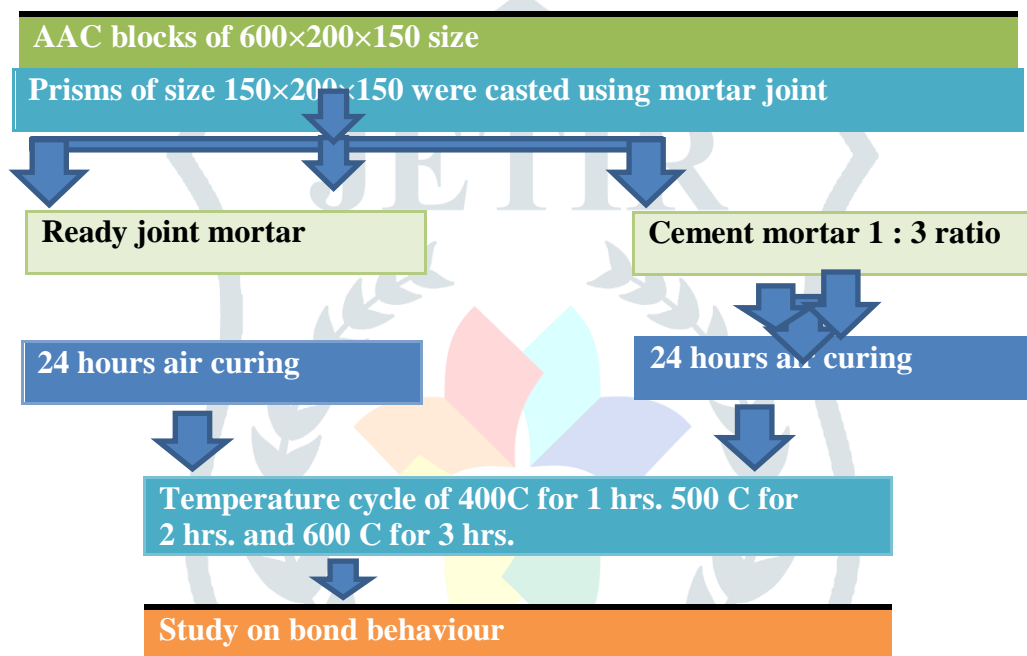
On strength behaviour of block specimens under varying temperatures Compressive strength test for all the specimens were conducted by placing them in compression machine and load applied perpendicular to the direction of the slices from which the cube thickness has been built up. For cubes which have been prepared in one piece, the direction of load shall be perpendicular to the direction of rise of the mass during production. The specimens were loaded at the rate of 0.5 to 2 kg/cm² in such a way that failure occurs within 30 seconds. After loading, the specimens were weighed and dried out at 105 +/- 5°C until constant weight is obtained as described in the procedure for determining the bulk density of aerated concrete blocks as per IS:6441 (Part I)-1972[6] (Vengalais, ShivakumarMangloor, & Talla Krishna Chaitanya Goud, 2009)

Following studies were carried out to know the initial trend of the temperature variation on AAC blocks in particular.

- Test specimens were cut to a size of 150mm×150mm×200mm from one entire block measuring 600×200×150 using hack saw blade.
- Total of 6 no's of specimens were cut out of which 3 specimens were sliced from the blocks, out of which 3 specimens were subjected to varying temperature of 600C, 1200C and 1800C with a duration of 60 min for each block using hot air and brought them to room temperature and tested individually for the load carrying capacity.
- Similarly, other 3 specimens were tested for its load carrying capacity at room temperature by immersing them immediately in water after subjecting them to temperatures 600C, 1200C and 1800C for 1hr. (Vengalais, ShivakumarMangloor, & Talla Krishna Chaitanya Goud, 2009)

B. Bond behavior of masonry joints with varying mortar ratios and thickness

Gives the flow chart for the strength behaviour of block specimens under varying temperatures.

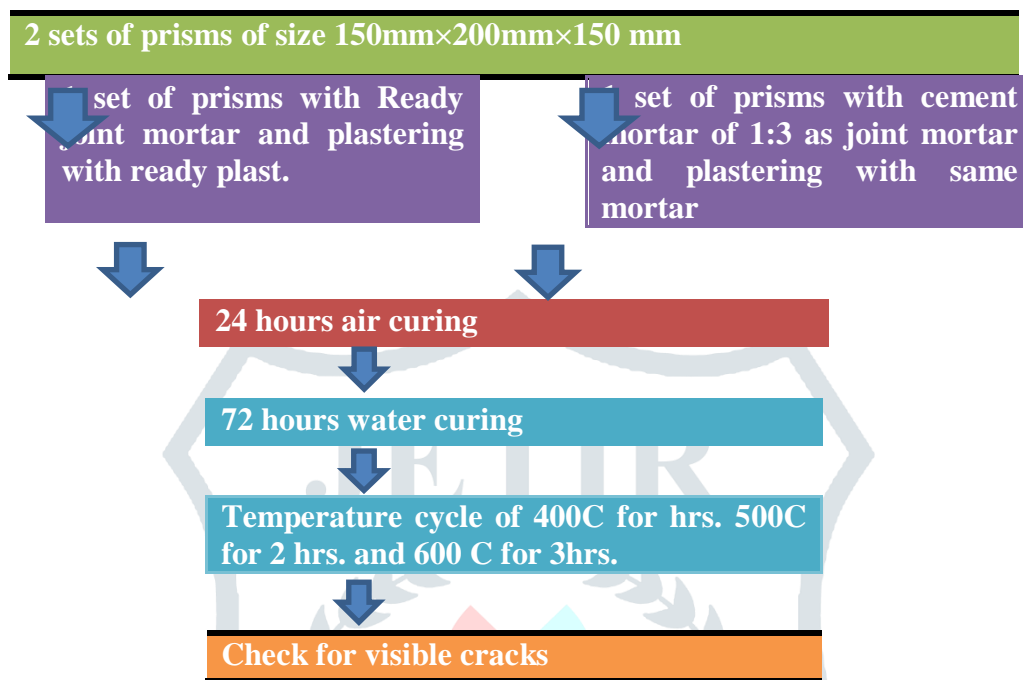


Prisms were casted for 2 sets of blocks using Cement mortar of 1:3 ratio and Ready joint mortar.

- Test specimens were cut to a size of 150mm ×150mm×200mm from one entire block measuring 600mm×200mm×150mm using hack saw blade
- Total 4 no's of prisms were casted out of which two prisms were casted using ready joint mortar. The other two prisms were plastered using cement mortar.
- The casted prisms were air cooled for first 24 hours followed by 72 hours of water cooling.
- Then cured prisms were subjected to varying temperature cycles of 400c for 1 hour followed by 500 c for 2 hours and 600 c for 3 hours in controlled hot air oven.
- The prisms were visually examined for the behaviour of bond with varying mortar types and thickness. (Vengalais, ShivakumarMangloor, & Talla Krishna Chaitanya Goud, 2009)

C. Crack behavior of prisms made with block specimens under varying temperature

Gives the flow chart for the strength behaviour of block specimens under varying temperatures behaviour of masonry joints with varying mortar ratios and thickness (Vengalais, ShivakumarMangloor, & Talla Krishna Chaitanya Goud, 2009)



Two sets of prisms were casted using Cement mortar of 1:3 ratio and ready joint mortar.

- Test specimens were cut to a size of 150mm ×150mm×200mm from one entire block measuring 600mm×200mm×150mm using hack saw blade
- Total of 4 no's of prisms were casted out of which two prisms were joined with ready joint mortar and plaster using ready plast. The other two prisms were joined using cement mortar of (1: 3) and plaster with the same cement mortar.
- The casted prisms were air cured for first 24hours
- Then cured prisms were subjected to varying temperature cycles of 400c for 1 hour followed by 500 c for 2 hours and 600 c for 3 hours in controlled hot air oven.
- After the completion of test program, the prisms were visually examined for the cracks. (Vengalais, ShivakumarMangloor, & Talla Krishna Chaitanya Goud, 2009)

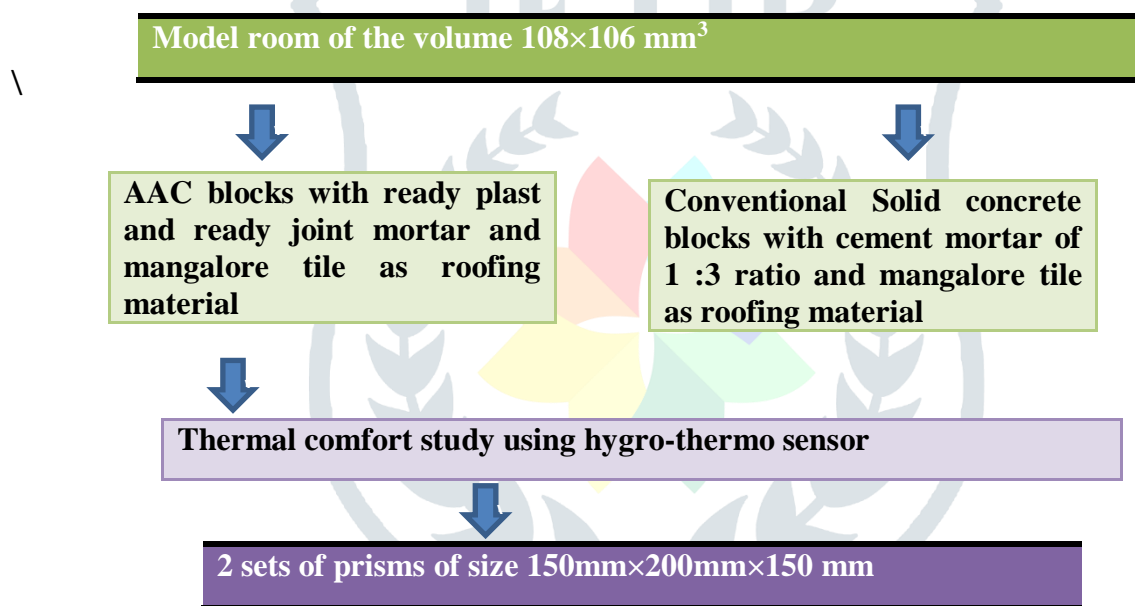
D. Thermal comfort studies on AAC blocks in comparison with solid concrete blocks:

Living comfort inside any building mainly depends on the “thermal comfort”. DIN ISO 7730 [7] deals with the research results related to thermal comfort . A large portion of the work in this area was done by a Danish scientist P. O. Fanger [8]. Thermal comfort mainly concerns the interior temperature of rooms,

maintaining and distributing it evenly, and the quality of the air (humidity rate, purity, healthiness). The solute on for comfort in winter and summer is a very high resistance thermal insulation of all surfaces (including the windows) combined with ventilation adapted to the season, perfect air tightness to avoid the parasite air input and the building's good thermal inertia.”[7,8] Optimal thermal comfort is established when the heat released by the human body is in equilibrium with its heat production. Fanger's comfort equation is derived from this fact. It creates a relationship between the activity (e.g. sleeping, running...) and clothing as well as the determining factors for the thermal surroundings, which are as follows (Vengalais, ShivakumarMangloor, & Talla Krishna Chaitanya Goud, 2009)

- Air temperature
- The temperature of the surrounding surfaces, this can also be summarised as the “radiant temperature”,
- Air speed and turbulence & air humidity

P.O. Fanger writes: “the more irregular the thermal field in a room is, the greater the expected number of dissatisfied people [7,8]. By keeping these points in view, a study was conducted to know the thermal comfort by constructing two model rooms one with AAC blocks and other with Conventional Solid Concrete Blocks. (Wahane, 2017)



For Temperature measurements, two model rooms were build. One was constructed using solid concrete blocks (SCB) and the other was constructed using autoclaved aerated concrete blocks (AAC). Table I gives the details of the materials used in both the model rooms used for thermal comfort studies. Thermo hygrometer was used to measure the temperature in both the model rooms. (Vengalais, ShivakumarMangloor, & Talla Krishna Chaitanya Goud, 2009)

Model Room	AAC	SCB
Blocks used	Autoclaved aerated concrete blocks	Conventional Solid cement concrete blocks
Mortar used for joints	ready joint mortar	Cement mortar 1:3
Mortar used for plastering	Ready plast	Cement mortar 1:3
Roofing material	Mangalore tile	Mangalore tile
Curing period	7 days	7days

TABLE I: Details of the materials used in both the model rooms.

2.4 RESULTS AND DISCUSSIONS

This section presents the compressive strength results of block specimens under varying temperature and bond behavior of masonry joints with varying mortar ratios and thickness and also includes the discussions based on the results obtained. Prisms were made with block specimens and crack behavior was observed under varying temperatures. Limited studies on thermal comfort behavior on scaled models constructed using AAC and conventional solid concrete blocks were also conducted. (Vengalais, Shivakumar Mangloor, & Talla Krishna Chaitanya Goud, 2009)

A. Strength behavior of block specimens under varying temperatures:

Table II presents the compressive strength results of AAC block specimens exposed to varying temperatures and a) air cooled b) water cooled immediately after subjecting to temperatures

Avg. wt. of the block	Temp. in $^{\circ}\text{C}$	Duration of exposure (min)	Curing Condition after exposing to temperature	Average Compressive strength of the Specimen (MPa)
3.3 Kg	Room temperature	-----	-----	4.5
	60	60	Air curing	3.36
		120	Air curing	4.49
		150	Air curing	4.29
	60	60	Water curing	3.30
		120	Water curing	3.40
		150	Water curing	1.52

TABLE II: Results of AAC block specimens at different temperatures

During the test program following observations were made:

- Average Compressive strength of the AAC block was 4.5MPa.
- For the study of strength behaviour both the sample of specimens were exposed to different temperatures for a constant duration of time and different cooling conditions no major and minor cracks were observed on the surface of both the set of specimens.
- When the comparison for strength was made with the controlled samples to the subjected blocks, with varying temperature not much variations were observed.
- In the case of set 2 specimens i; e specimens which were water cooled, around 20-30% reduction in strength was observed up to 1200c.
- Compressive strength of the blocks was drastically reduced when it exposed to 1500c followed by cooling the blocks to room temperature by immediately immersing in water. 35% of reduction in strength was observed.

- At 150 0c there is a slight color change in AAC block and color remained as pale yellow (Vengalais, ShivakumarMangloor, & Talla Krishna Chaitanya Goud, 2009)

B. Bond behavior of masonry joints with varying mortar ratios and thickness:

- To know the bond and mortar behaviour 2 set of prisms one with cement mortar and other with ready joint mortar was used at the joints.
- With a lean mortar mix of (1:6) of 2mm thickness the blocks were separated each other from prism due to poor bonding. Hence, 2mm thickness may not be recommended in case of lean cement mortar mix of 1:6. Based on the trials conducted with 2mm,4mm and 6mm thick cement mortar it was observed that a minimum of 4 mm thick CM is preferred in case of 1:6 proportion. (Vengalais, ShivakumarMangloor, & Talla Krishna Chaitanya Goud, 2009)

C. Crack behavior of prisms made with block specimens subjecting to temperature cycle:

- To know the crack behaviour, prisms were visually examined for appearance of cracks after subjecting to a temperature cycle i.e., 400C for 1hr and followed by 500C for 1hr and further 600C for 1hour.
- For the prisms plastered using ready joint mortar and ready plast mortar surface cracks started appearing after completing the 1 hr of exposure at 50 0c.
- Crack width of the same started increasing after exposing to 60 0 c for 1 hr on the plastered surface.
- Where in the case of cement mortar plastering of 1 :3 ratio, no surface cracks were seen on the surface of prisms till 50 0 c. But beyond this temperature, surface cracks appeared on the surface. However, this requires more test data.
- Table III gives surface crack behaviour of prisms with different mortar types and subjecting to a temperature cycle (Vengalais, ShivakumarMangloor, & Talla Krishna Chaitanya Goud, 2009)

Sl. No.	Type of mortar	Temp. in ⁰ c	Surface cracks observed over plastered surface		Width of the crack (mm)
			NO	YES	
1	Ready joint mortar and ready plast	40	√		--
		50		√	1.2
		60		√	2.5
2	Cement mortar 1 :3	40	√		--
		50	√		--
		60		√	1.2

TABLE III: Results of AAC block specimens at different temperatures

D. Thermal comfort studies of the AAC blocks in comparison with solid concrete blocks

- For Temperature measurements, two scaled models rooms were built. First scaled model was constructed using solid concrete blocks (SCB) and the other was constructed using AAC Blocks.

- Table IV gives the temperatures recorded using thermo hygro meter for both the scaled models
- Based on the limited studies conducted on scaled models AAC model shown better thermal comfort in comparison with the model with SCB i.e., cooler during day time by 1-20c . From table, it can be seen that the maximum temperature difference observed was 30C (Vengalais, ShivakumarMangloor, & Talla Krishna Chaitanya Goud, 2009)

	Avg. Temperature (⁰ C) recorded in scaled model		Difference in Temp. (⁰ C)	Rang e of temp (⁰ C)
	AAC blocks	SC blocks DAY		
1	29	31	2	1-2
	31	32	1	
	31	32	1	
2	29	29	0	0-1
	30	31	1	
	31	31	0	
3	28	30	2	1-2
	30	31	1	
	31	31	1	
4	29	31	2	1-2
	31	32	1	
	31	32	1	
5	29	31	2	0-2
	28	30	2	
	31	31	0	
6	28	30	2	0-2
	29	31	2	
	31	31	0	
7	27	29	2	2-3
	29	30	2	
	28	31	3	
8	29	29	0	0-1
	30	31	1	
	31	31	1	
9	28	30	2	0-2
	30	31	1	
	31	31	0	

TABLE IV: Temperature measurements of the scaled models

2.5 CONCLUDING REMARKS

The following conclusions have been drawn from the above study. Compressive strength of the blocks was drastically reduced when it is exposed to 1500c followed by cooling the blocks to room temperature by immediately immersing in water. Almost 35% of reduction in strength was observed. Hence, during fire situations it is not recommended to spray the water directly on the AAC Block surfaces. Joint mortar thickness of 2mm is not recommended in case of lean cement mortar mix of 1:6. A minimum of 4 mm thick CM is preferred in case of 1:6 proportion used as a mortar joint. Surface cracks on the plastered surface were observed

beyond 500 c temperature. However, this requires more test data. Based on the limited studies conducted on scaled models AAC model shown better thermal comfort in comparison with the model with SCB i.e., cooler during day time by 1-20c. (Vengalais, ShivakumarMangloor, & Talla Krishna Chaitanya Goud, 2009)

CHAPTER 3

Literature Survey and Detailed Objectives

3.1 Introduction

Many researchers have been investigating AAC blocks since last three decades due to their advantages. Considerable research has been carried out on estimating the strength of AAC by experimental methods and with the help of a few theoretical models. A number of experimental studies are described in this chapter; theoretical studies on modeling of AAC strength are also discussed. The connectivity or relation between various relevant properties of AAC and its masonry are presented. The study also emphasizes to understand the various factors responsible for overall strength of AAC building walls under various loading conditions. (Raj, 2020)

3.2 Physical Properties of Autoclaved Aerated Concrete (AAC)

Consideration of proper physical properties leads to conservative and capable building design and service. There are several physical properties of the AAC unit such as capillarity, permeability, porosity, shrinkage, thermal conductivity, thermal expansion, sound absorption, density, moisture content, water absorption (WA), sorption and initial rate of absorption (IRA) etc. Among these properties, the density, moisture contents, WA and IRA greatly affect the strength of AAC unit and masonry wall. In this Section, the relevant properties, much related to the strength of AAC masonry are discussed in brief. The connectivity or relation between various properties is also described. (Raj, 2020)

3.2.1 Density

The density of autoclave aerated concrete material is generally measured for oven dry mass. The density is generally in the range of 300–1000 kg/m³ (Narayanan and Ramamurthy 2000, Nambiar and Ramamurthy 2007, Aldolsun 2006, Hamad 2014, Qu and Zhao 2017). As per ASTM C1693 (ASTM 2017a) and RILEM (1993), the density of AAC is recommended to be in the range of 350–850 kg/m³ and 300–1800 kg/m³, respectively. Ferretti et al. (2015) reported the average density of 550 kg/m³ tested in Italy (Europe), while the density of AAC in India (Asia) ranges from 562–810 kg/m³ as reported by Researchers (Mallikarjuna 2017 and Bhosale et al. 2019). As per the standard procedure, the density of AAC block is evaluated based on the cubic specimen, extracted from top, middle and bottom portion of the block. The bottom cube shows the highest dry density followed by middle and top cube specimens. This difference arises because during the pre-curing process of manufacturing, the slurry in the mold expands or rises from

bottom to top in the direction parallel to the mold height (Ferretti et al. 2015, Mallikarjuna 2017 and Bhosale et al. 2019). AAC blocks of around 350 kg/m^3 density can be used for roofs, floors and load bearing walls. The density is mainly governed by the dosage of aluminum powder in the raw material mix during the production of AAC in the plant (Kunchariyakun et al. 2015 and Habib et al. 2015). The aluminum powder being an expansion agent in the mix increases the numbers of pores, thereby increasing the porosity and decreasing the density and compressive strength (Raj, 2020)

3.2.2 Moisture content, water absorption and initial rate of absorption

The AAC block contains moisture from the manufacturing process (CEB manual). The moisture may also accumulate in the material during construction or after the construction is completed i.e., from rain and condensation. The average moisture content of the AAC blocks lies in the range of 2–18% of the specimen weight (Bhosale et al. 2019). Kunchariyakun et al. (2015) reported that AAC in equilibrium with normal environment (65% relative humidity and 20°C), tends to have a moisture content of about 3% of volume. Bhosale et al. (2019) reported that the average water absorption (WA) of AAC lies in the range of 28–53%. The WA is the amount of water required to saturate the masonry unit; it is a measure of porosity. The water/moisture may migrate through diffusion or through capillarity or both. Because of higher porosity and water absorption of AAC, as compared with the normal brick/concrete, the surface treatment should be considered for the exterior surfaces of AAC. The mortar with three coats not exceeding 20 mm is used as the surface coating for the masonry wall. The unit moisture content and the water absorption (WA) play a key role in determining the bond strength of block-mortar interface. Highly absorptive specimens absorb more water from the adhesive joint and hence, reducing the masonry bond strength. In addition, the higher WA causes the damage to the wall finish as well as cracks on the plaster (Bhosale et al. 2019). IRA or suction is the amount of water absorbed per unit area per unit time, with SI units of $\text{kg.m}^{-2}.\text{min}^{-1}$. How quickly a masonry unit absorbs water from the mortar, is determined by IRA. The IRA of AAC ranged from $1.72 \text{ kg.m}^{-2}.\text{min}^{-1}$ to $4.91 \text{ kg.m}^{-2}.\text{min}^{-1}$. (Raj, 2020)

Masonry units are said to be highly absorptive when IRA is greater than $1.5 \text{ kg.m}^{-2}.\text{min}^{-1}$ and hence, should be moistened prior to laying for realizing better bond strength. High IRA for AAC units may result, poor brick-mortar bond for thin mortar with less water-cement ratio because of rapid suction of water by brick from mortar. High value of WA and IRA of AAC may result because of its highly porous nature. For a dry density range of $390\text{--}630 \text{ kg/m}^3$, the porosity value for AAC material has been reported to be 74–84% (Aldolsun, 2006). Too high and too low IRA not only affects the bond strength of brick-mortar interface, but also the durability and water-resistance of bricks. Hence, it is important to control the porosity, which is negatively correlated with the density of AAC. Both WA and IRA is the indicator of bonding potential of brick/block-mortar interface. In United Kingdom, the WA is used to specify the bonding potential, while in Australia, the IRA is used to specify the bond potential of brick-mortar interface (Lawrence et al. 1994). (Raj, 2020)

3.3 Strength of Individual AAC Unit

The strength of concrete is basically its ability to withstand various types of mechanical loads acting on it. The loads may be compressive, tensile, shear and flexural or their combinations; the strength corresponding to these loads are called compressive strength, tensile strength, shear strength and flexural strength, respectively. In this section, the different mechanical properties such as compressive strength, tensile strength and modulus of elasticity are discussed. Several factors affecting the mechanical properties of AAC are also described. (Raj, 2020)

3.3.1 Moisture content, water absorption and initial rate of absorption

The average value of compressive strength of AAC blocks range between 1.3–8.5 MPa for a density range of 400–700 kg/m³ (Hul et al. 1997, Narayanan and Ramamurthy 2000, Holt and Raivio 2005, Albayrak et al. 2006, Nambiar and Ramamurthy 2007, Aldolsun 2006, Hamad 2014, Qu and Zhao 2017, Mallikarjuna 2017 and Bhosale et al. 2019). The compressive strength of AAC strongly depends on its density and porosity. With increase of porosity and decrease of density, the compressive strength gets decreased. An increment of small-size pores leads to higher compressive strength. In other words, the refinement of pore- size distribution can lead to obtain both high porosity and high compressive strength. The utilization of coarser sand during the manufacturing of AAC also leads to higher strength of the final products. The compressive strength of AAC varies inversely with moisture content (Houst et al. 1983). There is an increase in strength on drying the aerated concrete to equilibrium with normal atmosphere. Hence, the strength tests are recommended on AAC material that has attained the equilibrium with the surroundings (Svanholm, 1983). The compressive strength of AAC block reduces by 20–25% as the moisture content increases by 5–10%, respectively. (Raj, 2020)

In addition to the porosity, dry density and moisture contents, the compressive strength also depends on the shape and size, direction of loading, age and characteristics of ingredients used during production. Habib et al. (2015) studied the compressive strength performance of aerated concrete by varying the aluminum powder content from 0.05% up to 0.25%. It was found that increase in the amount of aluminum powder decreases the compressive strength of aerated concrete. The presence of lower amount of aluminum powder tend to reduce the occurrence of aeration process that ultimately leads to the development of lesser amount of air voids, causing low expansion which finally yields hardened aerated concrete having lower porosity with higher compressive strength. On the other hand, inclusion of more aluminum powder promote the generation of higher amount of air bubbles trapped within the hardened aerated concrete forming higher expansion which finally leads to lower compressive strength. (Raj, 2020)

Alexanderson (1979) found that the compressive strength of aerated concrete, especially cements and lime mixing, increases with the increasing amount of hydrates and with decreasing porosity. The strength of hydration products, overall porosity and porestructure i.e., shape, size and the connectivity of the pores play a key role for governing the compressive strength of AAC. The water to solid ratio (W/S) is a critical

criterion for regulating the compressive strength of AAC. The W/S ratio is defined as the water to solid components of AAC (flyash, lime, cement, gypsum and aluminum powder) during production. Larger W/S ratio results in more microscopic pores and lower final strength (Narayanan and Ramamurthy 2000, Alexanderson, 1979). Ayudhya and Israngkura (2011) studied the compressive strength of AAC containing perlite aggregate and polypropylene fiber subjected to high temperature. It is concluded that compressive and splitting tensile strength of AAC containing polypropylene fiber is not much higher than those containing no polypropylene fiber. (Raj, 2020)

Several researchers have tested the compressive strength of AAC using different test specimens. Ferretti et al. (2014) investigated the compressive strength of AAC cube specimen of edge length 100 mm. They also performed the compressive strength test on AAC specimen of sizes and shape equivalent to actual AAC block, i.e., a rectangular block of size $625 \times 100 \times 250 \text{ mm}^3$. The strength of actual size AAC block specimen was 20% lower than that measured on cubic specimen. During the pre-curing at the time of manufacturing AAC, the slurry expands or rises from bottom to top in the direction parallel to the mould height. Hence, due to gravity, the bottom part of AAC is significantly denser and stronger than middle and top one. As a consequence, all the edges or corners of AAC specimen have different strengths. The cracks initiate near the weakest external corner. As the top part of AAC specimen is less dense, the crack initiates from the top part of AAC. (Raj, 2020)

Based on the tests conducted on 12 cubic samples, Mallikarjuna (2017) reported the average compressive strength of AAC block as 2.61 MPa. The compressive strength of AAC is relatively low as compared to the conventional brick/block used in the building construction. This encouraged Farid et al. (2017) to propose AAC-concrete sandwich composite to enhance its compressive strength. Compression tests were conducted on three sets of plain sandwich specimens, each with a different combination of concrete thickness and AAC thickness. The proposed composite had a higher compressive strength than normal AAC. The highest strength-to-weight ratio was found for 100 mm cubic specimen with concrete sheet thickness of 25 mm and 20 mm. The failure cracks were first appeared at the AAC-concrete interface. Hence, the interface bond strength enhancing techniques were also proposed by incorporating the groove at the AAC-concrete interface and by wrapping the block with wire mesh. The study revealed that the wire mesh provided a more effective bonding in comparison to plain sandwich block and grooved sandwich block. In general, AAC blocks are weak and soft as compared to normal burnt clay brick units (Kaushik et al. 2007) and fly ash brick units (Basha et al. 2014). The compressive strength of burnt clay brick and fly ash brick has been reported as 20.8 MPa (Kaushik et al. 2007) and 5.7 MPa (Basha et al. 2014), respectively (Raj, 2020)

3.3.2 *Moisture content, water absorption and initial rate of absorption*

The modulus of elasticity of AAC material is about one tenth of that of dense concrete and is a function of density and compressive strength. For a density range of $500 \text{--} 700 \text{ kg/m}^3$, the elastic modulus of AAC material has been reported as $1.1 \text{--} 2.8 \text{ GPa}$ (Alexanderson 1979, Narayanan and Ramamurthy 2000,

Aldolsun 2006, Hamad 2014, Ferretti et al. 2014, Qu and Zhao 2017, and Bhosale et al. 2019). In the study of Bhosale et al. (2019), the modulus of elasticity tested on the cubes of sizes 50 mm, 75 mm and 100 mm is reported to be in the range of 1.15–1.6 GPa. The elastic modulus can be positively correlated with compressive strength and density. The modulus of elasticity was found to vary from 220 to 820 times the compressive strength. Ferretti et al. (2014) reported a value of 1285 MPa evaluated with reference to stress level ranging between 2–33% of compressive strength. (Raj, 2020)

Based on 12 AAC cube specimens collected from M/S K.D. Infra, India, the average modulus of elasticity was 266 MPa (Mallikarjuna, 2017); it varied between 63 to 151 times of the compressive strength of AAC block. These results differ significantly with the results of other researchers (Alexanderson 1979, Narayanan and Ramamurthy 2000, Aldolsun 2006, Hamad 2014, Ferretti et al. 2014, Qu and Zhao 2017 and Bhosale et al. 2019). This may be due to the composition of raw material used to produce AAC block, individual strength of the raw material used and also differing climatic conditions. However, the tangent modulus obtained by the following empirical relation showed good agreement with the others (Raj, 2020)

$$E = k \rho_{\text{dry}}^{\sigma^{0.5}},$$

Where E_t is the tangent modulus (in MPa), ρ_{dry} is the dry density (in kg/m^3), σ is the compressive strength (MPa) and k is an empirical constant ranging between 1.5 to 2. (Raj, 2020)

3.3.3 Moisture Tensile strength of AAC unit

The tensile strength of AAC is normally about one quarter to one sixth of the compressive strength and is significantly affected by the moisture gradient within the test specimen (CEB manual). Valore (1954) reported the ratio of direct tensile strength to the compressive strength of AAC to be 0.15–0.35. Ferretti et al. (2014) evaluated the tensile strength and its statistical variability through a three-point bending test on normal and deep beams of the AAC. The tensile strength for 6 AAC beams of size $625 \times 100 \times 250 \text{ mm}^3$ has been reported to be between 0.56 MPa to 0.64 MPa. However, in case of 7 deep beams of size $625 \times 100 \times 750 \text{ mm}^3$, the tensile strength has been reported to be 0.69–0.83 MPa. The values agreed well with the design provisions suggested by researcher (Crisafulli, 1979). All the AAC beam specimens were characterized by brittle failure with main crack developed near the mid-span. However, deep beam showed a brittle failure characterized by the spreading of an inclined main cracks starting from the bottom of the specimen. The tensile strength increased with increase in the height of the AAC beam specimen. AAC is slightly stronger in flexural tension if the loads are oriented in parallel rather than perpendicular to the rising direction (Nambiar and Ramamurthy, 2006). (Raj, 2020)

Małyszko et al. (2017) evaluated the splitting test results both experimentally and numerically on the cylindrical and cubic AAC specimen. The splitting tensile test is a simple and effective method of evaluating the indirect tensile strength of the AAC specimen. The failure mechanisms were discussed based

on spatial finite element simulations and experiments with the digital image correlation and strain gauges. According to the theory of isotropic elasticity, the expression for the tensile strength for cylindrical AAC specimen is given in the form: (Raj, 2020)

$$\sigma_{\text{split}} = \frac{2(P_t)_{\text{max}}}{\pi DL},$$

where σ_{split} is the splitting tensile strength, $(P_t)_{\text{max}}$ is the measured peak load, D is the diameter of the specimen and L is the length of the specimen. The modulus of elasticity and Poisson's ratio have been calculated by fitting the theoretical solution into the displacement field. An average tensile strength of 0.39 MPa and 0.42 MPa were found for cylindrical and cubic specimen, respectively. (Raj, 2020)

Mallikarjuna (2017) reported the average splitting tensile strength of 0.26 MPa on a AAC specimen of size $200 \times 110 \times 75 \text{ mm}^3$. The test has been performed as per the ASTM C1006-07 (2013) on the specimen size equivalent to that of ordinary brick. Argudo (2003) studied the variation of splitting tensile strength with dry density and compressive strength of the AAC specimen. The linear regression analysis for splitting tensile strengths was carried out following ASTM C1006 test procedure. The empirical equations are given by

$$\sigma_{\text{split}} = 2\rho_{\text{dry}} - 10.3,$$

$$\sigma_{\text{split}} = 0.05\sigma + 30,$$

where σ_{split} and σ are the tensile splitting and compressive strengths in psi and ρ_{dry} is the dry density of AAC specimen in lb/ft^3 . The modulus of rupture has been found more in case of loading parallel to rise direction than that with loading in perpendicular direction. The modulus of rupture for loading in parallel to rise and perpendicular to rise direction has been found to be 1.25 MPa and 0.98 MPa, respectively. As per the RILEM recommendation, the modulus of rupture can be roughly estimated according to the formula

$$\text{MOR} = 0.27 + 0.21\sigma,$$

where σ is the compressive strength of AAC in MPa. The results obtained by several researchers differ a lot. This may be due to variation in specimens and testing standards. The raw material compositions and climatic conditions (humidity) of different regions can be also the reason for large deviation in results. Moisture content within the AAC specimens also affects the overall tensile strength. (Raj, 2020)

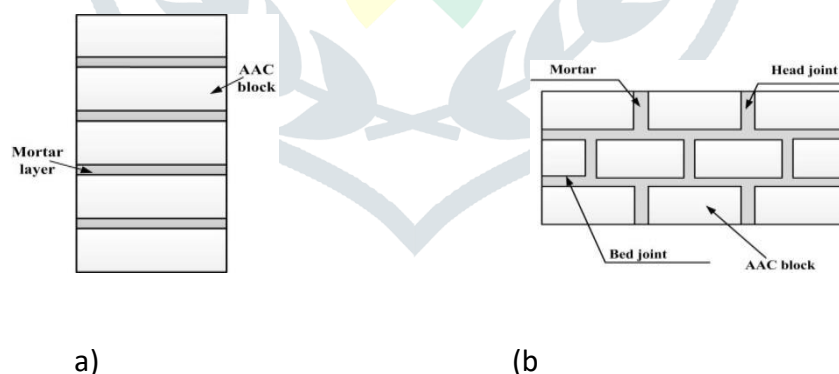
3.4 Mechanical Properties of AAC Masonry

Masonry is a nonhomogeneous, anisotropic and non-elastic material composed of two materials viz., unit and mortar/glue layer of different properties (Kaushik et al. 2007). The mortars or glues are generally stiffer than the AAC unit. The mechanical properties of AAC masonry are different from those of the individual

AAC unit specimen. The presence of joints such as bed joint and head joint (see Figure 2.1) in the AAC masonry or wall affects its overall strength. In this section, all the mechanical properties viz., compressive strength, tensile bond strength, shear bond strength and fracture energy of AAC masonry are discussed under the following sub-sections. (Raj, 2020)

3.4.1 Compressive strength of AAC masonry

The strength of brick-mortar masonry, loaded concentrically in the direction perpendicular to the bed joint is called its compressive strength (Crisafulli, 1997). In the masonry, different materials are distributed in a fixed interval and the bond between them is weak. The compressive strength of the masonry is generally investigated by testing prism specimens (Kaushik et al. 2007). The prism test specimen is the combination of 2-6 bricks units with required mortar layers stacked into one unit. Many researchers reported the prism strength or compressive strength of AAC masonry (Ferretti et al. 2015, Mallikarjuna 2017 and Bhosale et al. 2019). The compressive strength of the masonry prism is observed to lie between the strength of individual AAC unit and mortar. Bhosale et al. 2019) investigated the compressive strength of AAC masonry prism using 3 blocks stack-bonded with two layers of polymer based mortar of 2-5 mm thickness. The mean values of compressive strength and corresponding strain was found to be 2.12 MPa and 0.0018, respectively. A huge decrease (about 59%) in the compressive strength of masonry prism was found as compared to the compressive strength of individual AAC block. This may be due to the development of lateral stresses in the block and mortar layer. The lateral stresses are developed because of the differences in the mechanical properties (mainly elastic modulus and Poisson's ratio) of AAC unit and mortar material. (Raj, 2020)



Schematic drawing of AAC masonry for compression test (a) prism specimen and (b) masonry wallette

Although the overall compressive strength of masonry can be observed using masonry prism test, but the effect of bed joint and head joint (Figure 2.1 b) are not considered in this type of specimens. Sometimes, the masonry wallette/wall specimens are constructed to observe the effect of head joint and bed joint on the compressive strength of masonry walls (Ferretti et al. 2015). The direct test on the wall specimen itself can be considered as an actual strength analysis for compression. An average value of compressive strength on the AAC wall or masonry panel specimen has been observed to be 2.60 MPa. (Raj, 2020)

In general, the compressive strength of masonry depends on many factors such as mortar water retention,

water absorptions of masonry unit, strength of masonry unit, mortar/glue strength, mortar/glue thickness and workmanship (Crisafulli, 1997). The masonry strength decreases with the increase in water absorption of the brick unit. A very low value of water absorption can lead to a reduction in the compressive strength because of lack of water for necessary hydration for bond formation (Crisafulli, 1997). The excess water absorbed by the brick unit may result in lack of residual water essential for developing the strength of mortar. The masonry compressive strength can be increased by increasing the compressive and tensile strength of the brick units. The masonry strength is also related to the mortar/glue strength. The increase of mortar strength has significant influence on the compressive strength of masonry (Sarangapani et al. 2005). (Raj, 2020)

3.4.2 *Shear bond strength of AAC masonry*

The proper evaluation of the shear bond strength of a masonry unit is required for the design of any masonry panel when subjected to the lateral loads. The lateral loads get induced due to earthquake vibration, shaking and due to wind pressure on the wall surface. In the study by Bhosale et al. (2019), the shear bond strength of AAC masonry triplet made of polymer based mortar, has been reported to be 0.22 MPa. In general, the shear bond strength of the masonry depends on the brick porosity, initial rate of absorption of brick, surface roughness of brick, sizes of frog on the brick surface, chemical reactivity of mortar, characteristics of sand in mortar, water retention of mortar, mortar strength, presence of additives in the mortar and on pre-compression load (Groot 1993, Walker 1999, Sarangapani et al. 2005, Reddy et al. 2007, Reddy and Vyas 2008, Singh and Munjal 2017 and Mallikarjuna 2017). Some comments about these factors are presented here. The shear bond strength of masonry increases with the increase in the moisture content in the brick (Sinha 1983). A dry brick absorbs water from the mortar and hence, there may be the insufficient water available for the hydration of cement. The shear bond strength of masonry increases with the increase in the compressive strength of mortar (Rahman and Anand 1994 and Mallikarjuna 2017). The grading of sand also influences the shear bond strength. The sand graded as coarse-medium has shown the stronger bond strength between the brick and mortar (Sinha 1983). For adequate bond strength, an optimum amount of cementations material is required at the interface. However, insufficient amount leads to the adhesive failures at interface, whilst the excessive amount will lower the cohesive or tensile strength of mortar layer adjacent to the interface (Sugo et al. 2001). (Raj, 2020)

The AAC blocks are wire-cut as per the industrial practice, which results in smooth surfaces. When the two blocks with smooth surfaces are joined with conventional sand- cement mortar, a high shear bond strength is not attained (Mallikarjuna, 2017). The presence of frog in clay brick imparts higher masonry shear bond strength (Sarangapani et al. 2005, Reddy and Vyas 2007, Reddy et al. 2008, Singh and Munjal 2017). Mallikarjuna (2017) performed the shear bond strength test on triplet test specimen of AAC unit masonry using 5 different mortar grades (different proportions of sand and cement). The mortar grades used were 1:2, 1:3, 1:4, 1:5 and 1:6 corresponding to cement: sand. The tests have been carried for a pre-compression load of 0.1 MPa, 0.3 MPa and 0.5 MPa and without any pre-compression load. The shear bond strength was

found to increase with increase in compressive strength of mortar and with increase of pre-compression load. The behavior of AAC masonry bed joint and pre-compression has been observed and illustrated by the Coulomb's friction law. The relationship between shear bond strength (τ) and pre-compression stress (σ_p) is linear and is given by the following equation.

$$\tau = c + \sigma_p \tan \beta_j,$$

where c is cohesion i.e., shear bond strength of the brick-mortar interface when no pre-compressive stress is applied, σ_p Mathematically, the shear strength for the triplet test specimens is calculated as

$$\tau = \frac{P_{\max}}{2A},$$

$$\sigma_p = \frac{P_c}{A}$$

Where τ is shear bond strength in MPa, P_c is compressive load in N, P_{\max} is maximum shear force applied in N; and A is the cross-sectional area of the specimen parallel to the shear force or the bonding area in mm^2 . The average shear bond strength of AAC brick triplet specimen for 1:3 grade mortar have been reported to be 0.056 MPa, 0.226 MPa, 0.273 MPa and 0.40 MPa corresponding to pre-compression stress of 0 MPa, 0.1 MPa, 0.3 MPa and 0.5 MPa, respectively. Also, it was concluded that the shear bond strength of AAC masonry triplet increases with increase in the pre-compression stress. (Raj, 2020)

3.4.3 Tensile bond strength of AAC masonry

The resistance of masonry to tensile stress when subjected to out-of-plane loading is an important aspect for the safe design of masonry wall system. The tensile strength of masonry is primarily governed by the bond strength of brick mortar interface (Crisafulli1997). Several researchers studied the tensile bond strength of AAC masonry. Bhosale et al. (2019) evaluated the tensile bond strength of AAC brick masonry based on the Z-specimen tests and the failure patterns have been observed during the test. The AAC Z- specimen masonry was prepared using the polymer/block adhesive based mortar. (Raj, 2020) According to Khalaf (2005), the total joint strength can be obtained by linear stress distribution and parabolic stress distribution. Since the tensile bond strength calculated using the parabolic stress distribution is lesser than the value calculated using linear stress distribution, the assumption of parabolic stress distribution is safer and conservative. Bhosale et al. (2019) reported the average tensile bond

strength of AAC masonry using the linear stress distribution and parabolic stress distribution as 0.28 MPa and 0.22 MPa, respectively. Mallikarjuna (2017) performed the test on cross-couplet specimens followed by the calculation of mode-I fracture energy. The load–displacement curves obtained from tests were used for the calculation of tensile bond strength (Tensile strength of mortar-unit interface is given as

$$\tau_t = \frac{(P_t)_{\max}}{A}$$

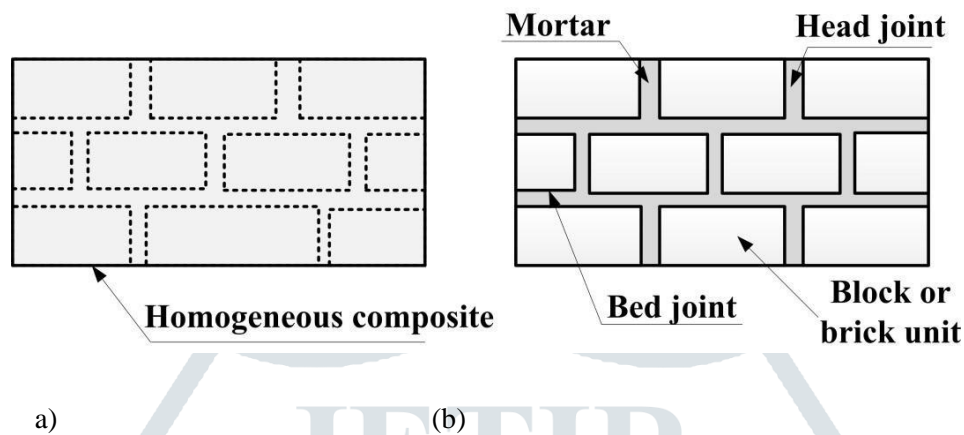
where τ_t is the tensile bond strength, $(P_t)_{\max}$ is the maximum value of the load applied, and A is the bonding area. The average tensile bond strength and the corresponding mode-I fracture energy were found to be 0.056 MPa and 0.01 N/mm, respectively. Ferretti et al. (2015) reported the tensile strength of AAC masonry beam and corresponding fracture energy in flexural loading using three-point bending test performed on 6 AAC small-scale masonry beams. The joint viz., head joint and bed material used for AAC masonry specimen preparation was grey glue of nominal joint thickness of 1.5 mm. The obtained tensile strength and fracture energy corresponding to 0° orientation of bed joint have been reported as 0.37 MPa and 0.007 N/mm, respectively. Similarly, for the bed joint inclination of 90°, it is reported as 0.30 MPa and 0.005 N/mm. The tensile strength test obtained on the AAC beam is the good realization of actual AAC masonry tensile strength. The presence of large number of bed joints and head joints in the AAC beam gives the actual representation of AAC masonry wall. (Raj, 2020)

3.5 Finite Element (FE) Modeling of Masonry Strength

Understanding the theoretical behavior of any engineering materials and system is very important. This can be achieved through numerical or computational studies. In last few decades, there has been a lot of study in developing a new method of modeling and analysis of masonry structures. The aim is to provide efficient tools for better understanding the complex behavior of masonry structures. The basic mechanical properties of the masonry are strongly influenced by its constituents namely, mortar and brick. Using the mechanical properties of unit, mortar and joint obtained from experiments, the behavior of masonry structure wall can be analyzed by Finite Element (FE) modeling. The FE Model has been developed to determine the strength, lateral displacement and stress distribution throughout the masonry wall system. Finite Element Method (FEM) is one of the most powerful tools for modeling a continuous masonry structure with the help of a number of complex elements. (Raj, 2020)

The modeling is done by converting the structure into simple finite elements. There are generally two approaches for FE modeling of masonry structures called homogeneous or macro modeling and heterogeneous or micro modeling (Lourenço, 1994). In homogeneous approach, the mortar joints and brick units are smeared into a uniform composite material with average property of individual brick and mortar (Figure 2.2a). However, mortar joint and units are considered separately in heterogeneous approach (Figure 2.2b). The micro-modeling regards the masonry as a heterogeneous material and

requires the determination of considerably higher number of parameters leading to expensive test (Bolhassani et al. 2015). Although the micro-modeling approach is more precise and can predict the local behavior of masonry, modeling becomes complicated by considering all the individual properties of masonry constituents. However, it needs more computational time. (Raj, 2020)



Modeling strategy of brick masonry: (a) macro-modeling and (b) micro-modeling

Lourenco (1994) used both micro modeling and macro modeling to study the behavior of masonry wall. The elastic model is used to represent the behavior of brick while the gradual softening model is used to represent the interface element. A three-dimensional FEM model using concrete damage plasticity (CDP) model for a partially grouted wall was developed by Minaie et al. (2010). Sejnoha et al. (2008) simulated a diagonal compression test using a continuum model for mortar and contact elements for the stone mortar interface. The results were promising but the model did not account for the gradual loss of cohesion. Alberto et al. (2011) characterized the mechanical behavior of interface and predicted the de-bonding phenomena between brick and mortar through cohesive crack model. (Raj, 2020)

Zhang et al. (2017) developed a detailed micro modeling method for the modeling of diagonal compression test for historical stone masonry structure using extrinsic cohesive element. Kowalewski and Gajewski (2015) determined the failure modes in the brick walls using a cohesive element approach. The micro modeling approach with the application of cohesive elements to describe the mortar joint was used in the analysis. Cohesive zone model was used for modeling the unit mortar interface. Since there is no any separate constitutive model for the finite element analysis of behavior of AAC beam or AAC masonry wall, many researchers (Ferretti et al. 2014, Ferretti et al. 2015, Mallikarjuna 2017 and Małyszko 2017) adopted the macroscopic anisotropic constitutive model already developed for ordinary masonry (Sejnoha et al. 2008, Minaie et al. 2010, Alberto et al. 2011, Kowalewski and Gajewski 2015 and Zhang et al. 2017). (Raj, 2020)

3.5.1 Concrete damage plasticity (CDP) for material modeling

The behavior of the masonry can be simulated in a commercial available FEM package such as ABAQUS using the CDP model, which can be used for concrete and other brittle materials (ABAQUS 6.13 Manual). The failure is caused by cracks in tension and crushing in compression. The concrete damage plasticity

provides a general capability for modeling concrete and other quasi-brittle materials in all types of structures (beams, trusses, shells, and solids). In CDP model, the evolution of the yield (or failure) surface is governed by two hardening variables viz., compressive equivalent plastic strain (ε^p) and tensile equivalent plastic strain (ε^p), which are linked to failure mechanisms under compression and tension loading, respectively. The stress-strain behavior under uniaxial tension follows a linear elastic relationship until it reaches the failure stress (σ_{t0}). The stress corresponding to the onset of micro-cracking in the concrete material is the failure stress (ABAQUS 6.13 Manual). The formation of micro-cracks with a softening stress-strain response induces strain localization in the structure of concrete. However, under the uniaxial compression loading, the response is linear until it reaches the initial yield stress (σ_{c0}). The response is typically characterized by stress hardening followed by strain softening beyond the ultimate stress (σ_{cu}) in the plastic region. The uniaxial stress-strain curve can be converted into stress versus plastic-strain curves by ABAQUS from stress versus plastic strain data. Thus, (Raj, 2020)

$$\sigma_t = \sigma(\varepsilon_t^p, \dot{\varepsilon}_t^p, f, \theta), \quad \sigma_c = \sigma(\varepsilon_c^p, \dot{\varepsilon}_c^p, f, \theta)$$

where the subscripts t and c indicate tension and compression, respectively. ε^p and $\dot{\varepsilon}^p$ are the equivalent plastic strains, $\dot{\varepsilon}^p$ and $\dot{\varepsilon}_c^p$ are the equivalent plastic strain rates, f_i (for $i = 1, 2, 3, \dots$) are the other predefined field variables and K is the temperature. (Raj, 2020)

When the concrete specimen is unloaded from any point on the strain softening branch, the stiffness decreases. The elastic stiffness of the material seems to be degraded or damaged. The elastic stiffness damage is characterized by two damage variables, d_t (for tension) and d_c (for compression), which are the functions of the plastic strains, temperature and field variables. The damage variables can be varied from 0 to 1. (Raj, 2020)

$$d_t = d(\varepsilon_t^p, K, f); \quad 0 \leq d_t \leq 1$$

$$d_c = d_c(\varepsilon_c^p, K, f); \quad 0 \leq d_c \leq 1.$$

For undamaged materials, the damage variable is 0, whereas 1 indicates the total loss of strength

(ABAQUS 6.13 Manual). Letting E_0 as the initial or undamaged elastic stiffness of the material, the stress-strain relations under uniaxial tension and compression become (Raj, 2020)

$$\sigma_t = (1 - d_t) E_0 (\varepsilon_t - \varepsilon^p)^I,$$

$$\sigma_c = (1 - d_c) E_0 (\varepsilon_c - \varepsilon^p)^I.$$

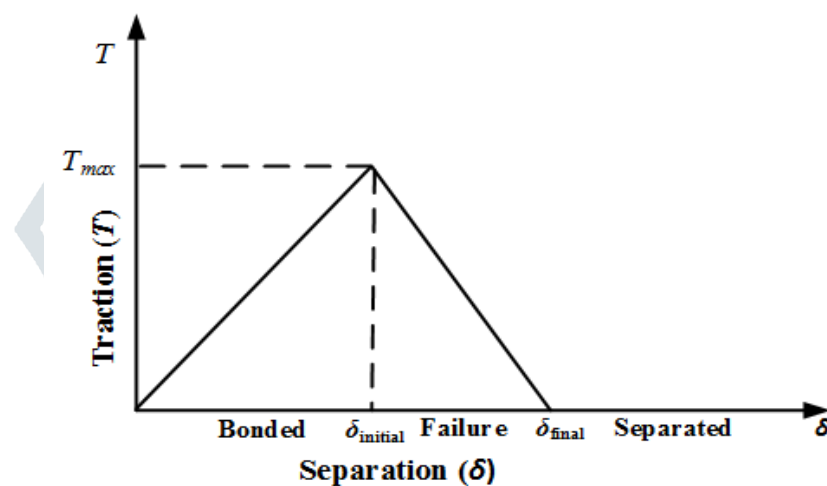
A non-associative flow rule is considered to define the plastic strain rate in CDP model. The multiple-hardening Drucker-Prager type surface is adopted as a yield surface. The yield surface is governed by the parameters such as dilation angle (φ), ratio of biaxial compressive strength to the uniaxial compressive strength (f_{b0}/f_{c0}) and a constant k (Lubliner et al. 1989, van Zijl et al. 2004 and Daltri et al. 2019). The dilation angle or dilatancy is basically the measure of change in the volumetric strain with respect to the changes in shear strain. The dilation angle defines the amount of plastic volumetric strain induced in the body during the plastic shear. The constant k is the ratio of second stress invariant on tensile meridian to that on the compressive meridian at the failure point. The tensile and compressive meridians are the intersection curves between the plane (meridian plane) containing the hydrostatic axis and the failure surface (Chen, 2007). (Raj, 2020)

3.5.2 Cohesive Zone Modeling

Cohesive zone (CZ) models are widely used to investigate the behavior of interfaces between any two materials. This model, introduced by Dugdale and Barenblatt (1960), has attracted a growing interest to describe the failure and delamination process for composite materials in details. The cohesive interaction is the function of displacement or separation between the edges of cracks. The CZ model is generally applied to concrete and cementitious composites but can also be used for other materials. The application of CZ model may widen the knowledge of material properties and more powerful computer programs. (Raj, 2020) Previous researches have studied the parameters that affect the cohesive interaction performance for brittle materials. They have concluded that the mechanical behavior of cohesive elements can be defined by three methods: (1) uniaxial stress-based, (2) continuum-based and (3) traction-separation constitutive model. In this work, the third method is used. The traction-separation model represents the corresponding initial separation caused by pure normal stresses, in plane and out of plane shear stresses. The Coulomb frictional contact behavior is applied to the traction-separation model by introducing a coefficient of friction (μ), which prevents components penetration, especially for the normal contact behavior. For this study, surface-to-surface contact is chosen and the contacting properties for the tangential and normal behavior are specified. This type of contact is generally used to describe the behavior of two deformable surfaces connecting together. This focuses all the damage mechanisms in and around a crack tip on the interface, leading to a constitutive relation between the traction and opening displacement (separation). The crack

initiation is related to the cohesive strength, also called the maximum traction on the traction separation law. The variation in traction in relation to separation or displacement is plotted as a curve and is called the traction-separation curve, as illustrated in Figure 2.3.

When the area under the traction-separation reaches the fracture toughness, the traction declines to zero and new crack surfaces are generated. The crack initiation is related to the cohesive strength, also called the maximum traction on the traction separation law. From Figure 1 it can be observed that the material is initially bonded and the failure occurs after the maximum traction is reached, beyond which the traction starts decreasing. (Raj, 2020)



Cohesive zone modeling relates the relative displacement (“opening” δ) of two associated points of the interface to the force per unit of area (“Traction” T) needed for separation. A difference is made between normal (n) and tangential (t) direction. Hence, the cohesive zone law comprises two parameters i.e., $T_n(\delta_n)$ and $T_t(\delta_t)$. The cohesive zone laws can be uncoupled or coupled (Bolhassani et al. 2015). In an uncoupled cohesive zone law, the normal/tangential traction is independent of the tangential/normal opening, while both normal and tangential tractions depend on both the normal and tangential opening displacement in case of coupled cohesive zone law. Uncoupled laws are intended to be used when the debonding process occurs under normal (mode-I) or tangential (mode-II) loading. The majority of cohesive zone laws have a partial coupling between normal and tangential directions, which is achieved by introducing coupling parameters in the model. A large variety of cohesive zone laws are available in literature, e.g., (a) polynomial model, (b) piece-wise linear model, (c) exponential model and (d) rigid linear model. (Raj, 2020)

The shear strength or bond strength of the masonry depends mainly on the interface between unit and mortar. The masonry interface modeling can be done using Cohesive Zone Modeling (Zhang et al. 2017). Cohesive zone model (CZM) can be used to predict the local fracture initiation and continued propagation in a material. It offers an alternative way to analyze failure along material interfaces. The CZM can be employed in FE analysis by relating the traction to displacement at interfaces. (Raj, 2020)

Ramamurthi et al. (2013) studied the delamination between polyethylene terephthalate (PET) and

polyvinyl chloride layers in polymer coated steel using two approaches to model cohesive zone for delamination viz., elemental cohesive zone model (ECZM) and surface cohesive zone model (SCZM). ECZM is a method for predicting the delamination process between the interface of bonded surfaces. However, SCZM is particularly used for zero or very thin interfaces, where the thickness effect is considered. The SCZM was found to be more desirable because of the advantages of reduced computational time, fewer input parameters and easy modeling (Ramamurthi et al. 2013). In this study, unit-mortar interface is modeled by adopting the surface based cohesive zone model. Turon et al. (2007) determined various constitutive parameters such as interface stiffness coefficient, length of cohesive zone for the simulation of delamination. The equation for the selection of interface stiffness parameter was derived. The expression to adjust the maximum interfacial strength used in the computations with a coarse mesh was presented. (Raj, 2020)

Ferretti et al. (2014) performed an inverse extended finite element (XFEM) analysis to calibrate a proper cohesive law suitable for the AAC material. The XFEM is basically an extension of conventional FE method based on the concept of partition of unity, which takes into account the discontinuous structure of displacement field. The XFEM eases the difficulties in solving problems with localized features e.g., presence of main crack that are not efficiently resolved by mesh refinement. Moslemi and Khoshnavan (2015) proposed a new test methodology to determine the cohesive strength of the composite laminates. The various cohesive parameters such as cohesive strength and separation energy for mode I inter-laminar fracture of E-glass/epoxy woven fabric was computed from the experimental tests. The results from the simulation were compared with experimental tests to confirm the adequacy of normal cohesive strength. Kowalewski and Gajewski (2015) determined the failure modes in the brick walls using cohesive element approach. The micro-modeling approach with the application of cohesive elements to describe the mortar joint has been used in the analysis. Małyszko et al. (2017) simulated the splitting test on cylindrical and cubic AAC specimens under the displacement control using the Mohr-Coulomb constitutive model of isotropic plasticity with the yield function expressed in terms of principal stress as (Raj, 2020)

$$f(\sigma, k) = \frac{1}{2} (\sigma_1 - \sigma_3) + \frac{1}{2} (\sigma_1 + \sigma_3) \sin \theta - c(k) \cos \theta, \text{ for } \sigma_1 \geq \sigma_2 \geq \sigma_3,$$

where $c(k)$ is the cohesion function of the internal state variable k with constant friction angle (θ), which is described by the hardening/softening diagram. Ferretti et al. (2015) used the experimental results to calibrate a well-known macroscopic anisotropic constitutive model already developed for ordinary masonry. The behavior of AAC masonry and full-scale AAC wall were simulated for both tension and compression. Two different failure criteria were adopted for compression and tension, respectively “Hill-type” and “Rankine-type”. Ferretti et al. (2015) concluded that the numerical anisotropic models proposed for traditional masonry can also be used for AAC masonry, if calibrated properly. Mallikarjuna

(2017) carried out a two dimensional linear elastic finite element analysis of a masonry shear wall under a pre- compression load of 0.1 MPa. The aim was to study the normal stress and shear stress distribution in masonry units and AAC unit-mortar bond interface assuming plane-stress condition. The potential failure mechanism and collapse load were estimated from the analysis. It was concluded that the simplified micro-modeling is a convenient method for finite element modeling of the masonry shear wall. The stiffness of the wall depends mainly on brick-mortar interface bond strength rather than the strength of the mortar (Mallikarjuna 2017) (Raj, 2020)

3.6 Major Gaps in the Literature

The information gathered from the review of published literature reveals a few research gaps and possibilities remaining for further investigation. The gaps found from the literature are summarized as follows:

- All the previous literatures are dedicated to study the mechanical properties of AAC masonry made of AAC block having smooth surfaces. However, the effect of surface roughness was not studied.
- The AAC blocks are wire-cut as per the industrial practice, which results in makes all the six surfaces smooth. No study was done to alter the bed face of AAC and feasibility of its implementation in the manufacturing industry.
- No researcher reported the study on enhancing the bond strength of AAC masonry by altering the unit surface characteristics.
- No researcher discusses the effect of mortar strength on the strength of AAC masonry.
- Various joining materials are used to form the AAC masonry such as conventional sand cement mortar and polymer modified mortar. No researcher studied the strength of AAC masonry using different joining materials.
- The nature of lateral stress developed in the block and mortar due the application of axial stress on AAC masonry for compression load is not presented till date.
- The joint thickness also affects the strength of ordinary (clay brick) masonry. In spite of it, the influence of mortar or glue thickness on the overall strength of AAC masonry is not present in the literature. (Raj, 2020)

3.7 Detailed Objectives of the Present Thesis

Based on literature survey, the main objective was defined as design and development of proper bonding mechanism for individual AAC block units in wall system of a structure. To accomplish the main objective, four sub-objectives were adopted, which are also the objectives of the present thesis. The detailed objectives are as follows: (Raj, 2020)

3.7.1 Evaluation of mechanical properties of autoclaved aerated concrete (AAC) block and its masonry

The first objective of this thesis is the experimental evaluation and statistical analysis of useful mechanical properties of AAC and its thick mortar (a mixture of cement, sand and water) based masonry. The following important physical properties of AAC blocks are evaluated: moisture content, initial rate of absorption, water absorption, dry density, compressive strength and tensile strength. For AAC masonry, the following properties are evaluated: compressive strength based on prism specimen test, tensile bond strength based on cross couplet specimen test and shear bond strength based on triplet specimen test. A simple analytical model is also proposed to evaluate the elastic modulus of masonry prism. The results indicate that there is a positive correlation between the strength of mortar and AAC masonry. The strength of AAC masonry increased with an increase in the strength of mortar. During the strength test of AAC masonry, the failure patterns were studied. The block mortar interface failure was observed in most of the cases during the masonry bond strength test. A positive correlation was observed between masonry bond and compressive strengths. Further, a comparison of strengths of masonries made of AAC block and clay brick is presented. At the present level of manufacturing, AAC masonry cannot compete with clay brick masonry in terms of strength alone. (Raj, 2020)

3.7.2 Compressive and shear bond strengths of grooved autoclaved aerated concrete blocks and masonry

The second objective of the present thesis asserts that the shear bond strength of AAC masonry can be enhanced by using grooved AAC blocks. The compressive strength of the grooved AAC block as well as the shear bond and compressive strengths of the masonry have been investigated experimentally and compared with conventional AAC blocks and masonry. The study clearly demonstrated the superiority of grooved AAC blocks to conventional AAC (Raj, 2020)

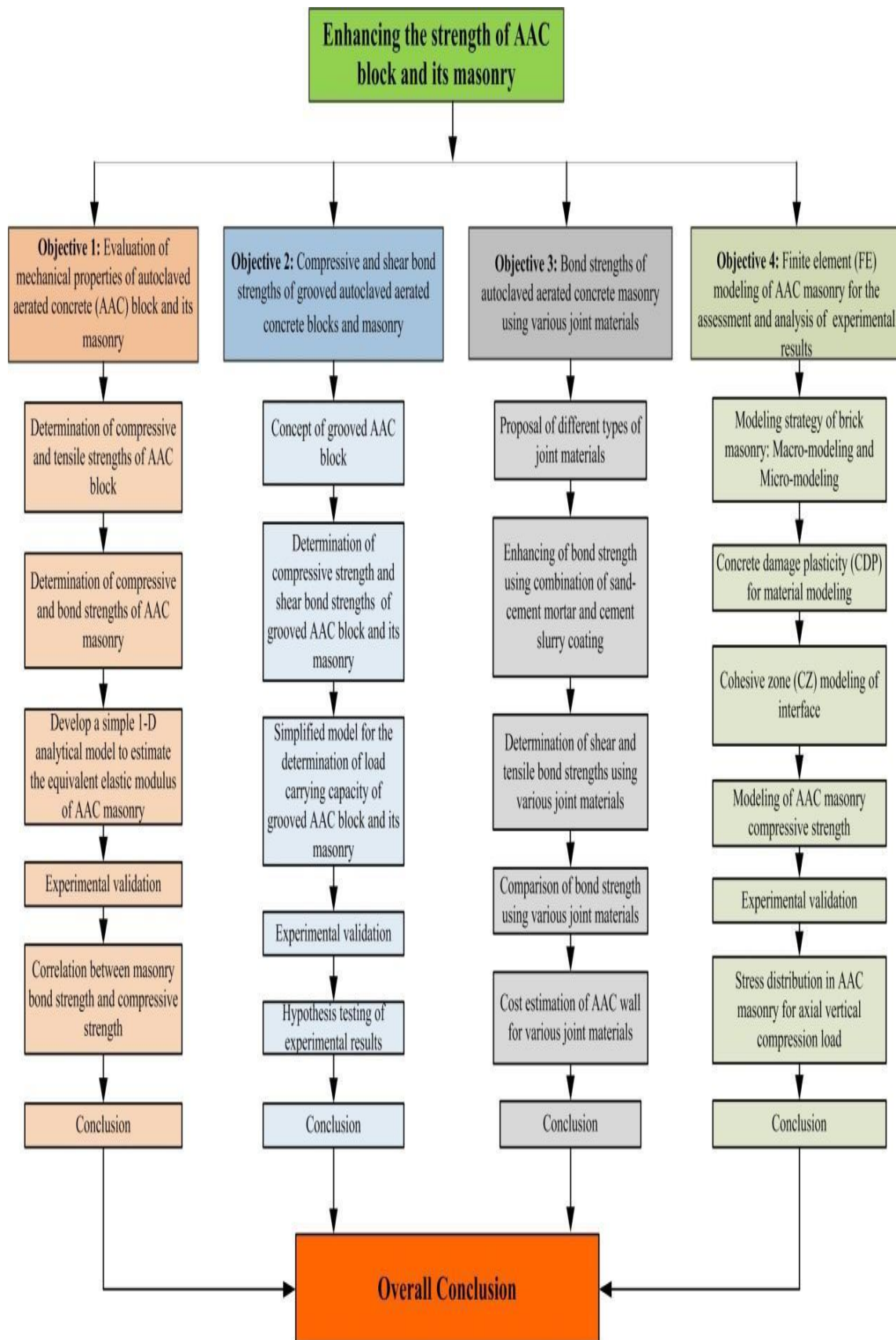
blocks. Simple analytical models have been developed to estimate the masonry compressive and shear bond strengths. Analytical models are capable of obtaining lower, upper and most likely estimates of strengths. Significance tests have been carried out to support the findings. (Raj, 2020)

3.7.3 Bond strength of autoclaved aerated concrete masonry using various joint materials

The third objective of this thesis investigates the bond strength of AAC block-mortar interface made of ordinary sand-cement mortar of different compositions and polymer modified mortars. A method of improving the bond strength (both tensile and shear) of ordinary sand-cement mortar without altering the block surface characteristics is proposed. In this method, the block surfaces are coated with a thin cement-slurry coating before applying a thick sand-cement mortar. For all types of interfaces, the shear bond strength of the masonry was studied using a triplet test, while the tensile bond strength was determined based on a cross-couplet test. The failure patterns during the bond strength tests were studied. Subsequently, costs were estimated for AAC walls of different types of interfaces. Considering the bond strength as well as cost, using a weak mortar along with cement-slurry coating was found superior to the ordinary sand-cement mortar and polymer modified mortar. (Raj, 2020)

3.7.4 Finite element (FE) modeling of autoclave aerated Concrete masonry for the assessment and analysis of experimental results

The fourth objective deals with the finite element modeling of AAC masonry for the estimation of compressive strength. For a load bearing structure as well as framed structure, in-plane compression is an important mode of failure in the masonry walls. In this work, the finite element micro-modeling, governed by plastic-damage constitutive relation in tension and compression, has been used to model the AAC block and mortar, while cohesive zone modeling strategy is adopted to model the block-mortar interface. The developed model has been used for the estimation of compressive strength of AAC masonry. The nature of lateral stress developed due the application of axial stress is discussed. The comparative study on stress distribution in AAC block and clay brick masonries is also presented. The results obtained from modeling have good agreement with the experimental results. (Raj, 2020)



3.8 COMPARATIVE ANALYSIS OF (AAC) WITH CONVENTIONAL FIRED BRICK

➤ *ENERGY EFFECTIVENESS*

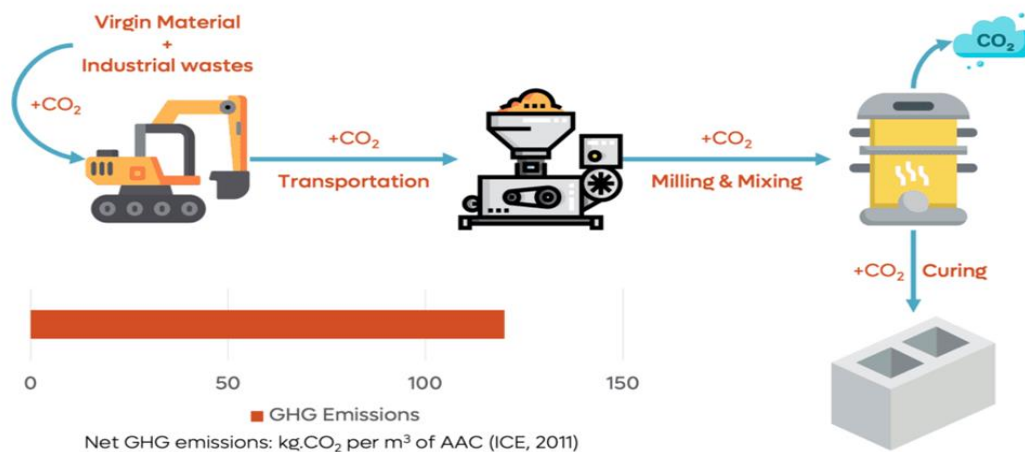
Initial embodied energy (kWh/m ³ of materials)	Carbon emission (Kg of CO ₂ per m ² carpet area)
AAC Blocks consume approx. 70% less energy than Clay bricks. AAC block produced (50-100)kWh/m³	Fired clay brick pollute 8 time than AAC block. AAC block produces 23.58 kg of CO ₂ /m ²
Country fired bricks (900-1000) kWh/m³	Country fired bricks = 190 Kg of CO ₂ /m ²

The initial **embodied energy** of AAC is in general less than other building materials.

- AAC block consumes 70% times less energy than country fired bricks (Indian Average).

Carbon dioxide emission is in general less than other building materials.

- AAC emits 8 times less carbon dioxide than country fired bricks.

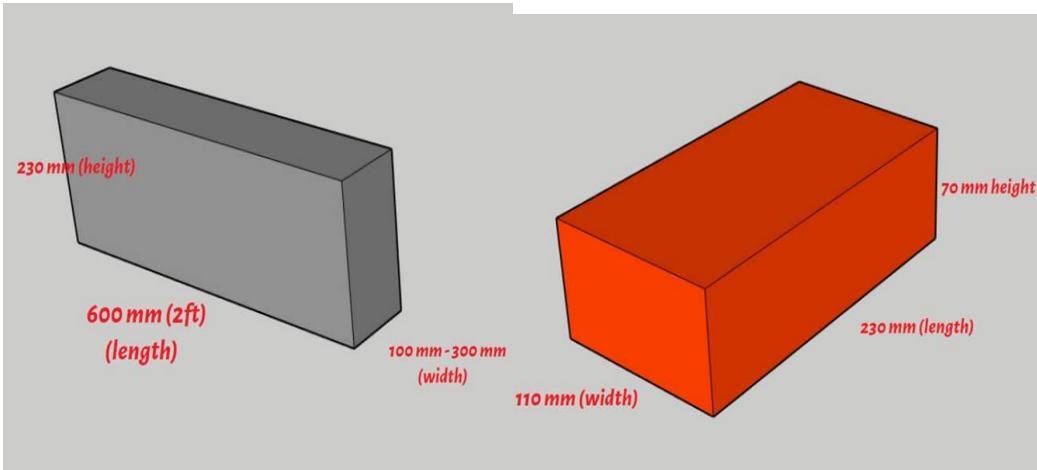
➤ *STRENGTH*

- Compressive strength of brick = 2.6 kg/mm²
- Compressive strength of AAC = 3.5 kg/mm²

➤ *COST EFFECTIVENESS*

- Less water is needed in for curing
- Less mortar is required and it is cheaper.
- 5% of waste against 10% for country fired bricks

3.9 COMPARATIVE ANALYSIS (TECHNICAL PROPERTIES)



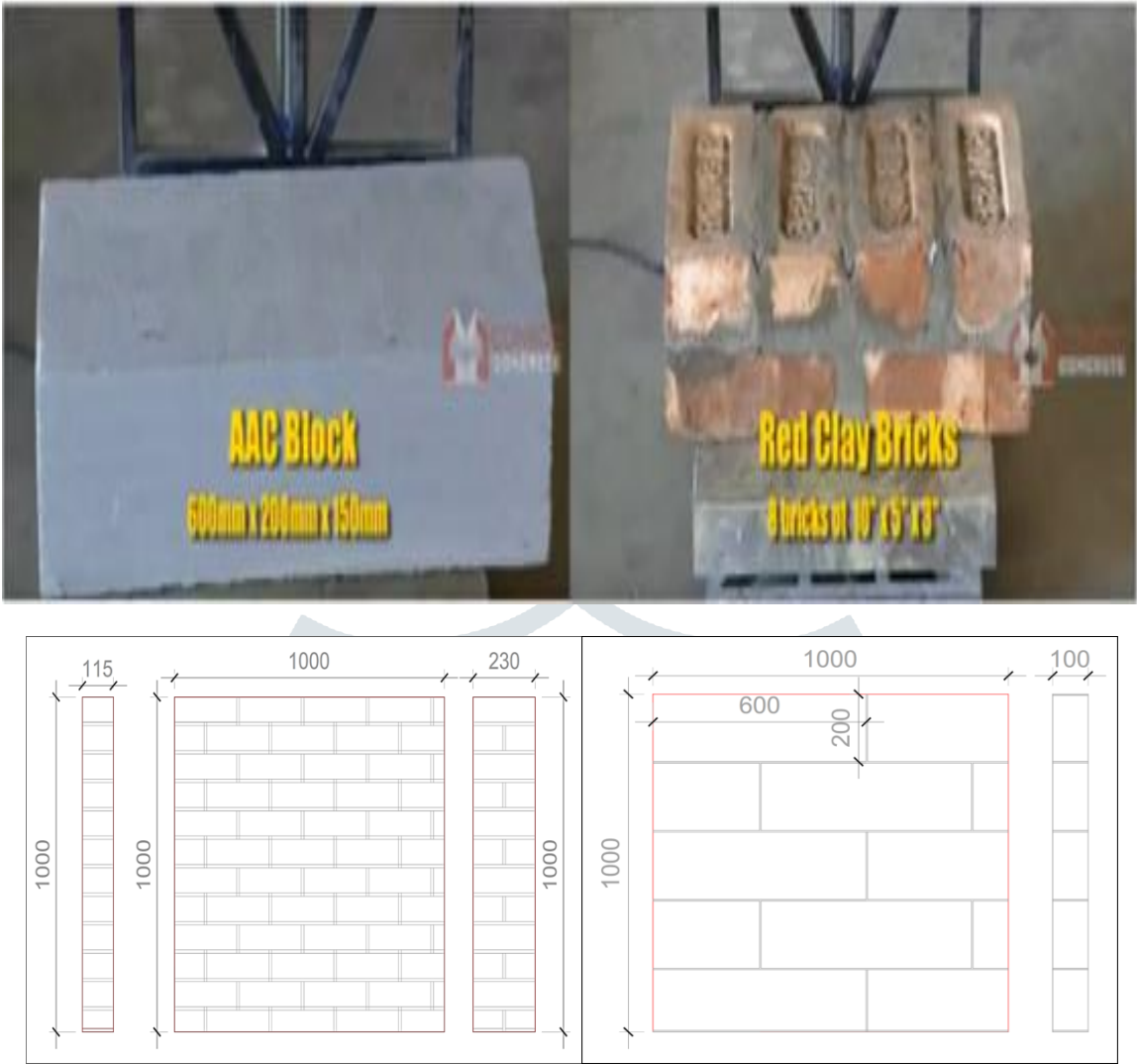
AAC BLOCK DIMENSIONS

RED CLAY BRICK DIMENSIONS

(aac-blocks-vs-red-bricks-comparison)

3.9 COMPARATIVE ANALYSIS- AAC Blocks VS red Bricks (Construction Speed)

S. NO.	PARAMETERS	CONVENTIONAL BRICK	AAC BLOCKS	Inferences
1	Area	Area of brick is 9 inch x 3 (230 mm x 70 mm) = 0.0161 sqm No of bricks = 9 sqm / 0.0162= 555 bricks (230 x 110 x 70 mm) size	Area of block = 24 inch x 9 inch (600 mm x 230 mm) = 0.138 sqm Wall area = 3m x 3 m = 9 sqm No of blocks = 9 sqm/0.138sqm = 65 blocks (600 mm x 230 mm x 100 mm) size	
2	Joints	Total mortar joints 170 r/ mt for 4 inch wall & 210-220 r/sq.mt. for 9 inch wall	Total mortar joints 62 r/ sq.mt. (approx.)	
	Weight	Weigh of brick = 3-3.5 kg (approx.)	Weight of an AAC block 9 kg	
3	Replacement		1 no 9 inch block = 8-9 bricks	



(aac-blocks-vs-red-bricks-comparison)

3.10 COMPARATIVE ANALYSIS- AAC Blocks vs red Bricks (Cost Saving and Labour Handling)

S. NO.	PARAMETERS	CONVENTIONAL BRICK	AAC BLOCKS	Inferences
1.	Speed & finishing	Red bricks are locally made and are irregular with less dimensional accuracy. Bricks are very difficult to place, level, and plumb.	AAC blocks are factory-made and possess dimensional accuracy. They are easy to place and plumb	
2.	Mixing	Brickwork is done by site mixed mortar and has to be a minimum of 10 mm. The mortar thickness is high in the case of brickwork.	AAC blocks mostly use block adhesive for bonding and are available in ready mix packs. The thickness of mortar joints ranges between 3-5 mm.	

3.	Curing	Bricks have to be soaked in water before using it in works. Moreover, 7-day curing has to be done on brickwork. This requires setting up of curing infrastructure, and labor involvement.	AAC blocks do not require any pre-curing. AAC block masonry joints are air-cured and need not require any curing.	
4.	Labour saving in mortar mix	Brickwork uses site mix mortar that involves handling, mixing, and conveying of raw materials, and mortar.	AAC blocks use ready-mix bonding adhesive as jointing material. They are available in 25-30 kg packs and to mix with water before use.	

(aac-blocks-vs-red-bricks-comparison)

3.11 COMPARATIVE ANALYSIS- AAC Blocks vs red Bricks (Mortar Required)

ANALYSIS OF MORTAR REQUIRE FOR 1 CUM BRICKWORK		
Volume of 1 brick (without mortar)	0.23X0.1X0.075	0.001725 cum
No. of brick required without mortar	Volume of 1cum brick work/Volume of brick without mortar 1 / 0.001725	580 Nos.
Add 10 mm mortar thickness		
Volume of brick with mortar	0.24X0.11X0.085	0.002244 cum
No. of brick required with mortar	Volume of 1cum work/Volume of brick with mortar 1/0.002244	446 Nos.
Quantity of mortar for 1 cum work		
Quantity of mortar volume	Volume of Brick work – (Volume of AAC Block without mortar x Number of AAC Block required with mortar) 1- (0.001725 X446)	0.230 cum.

- There is need of 446 red brick and 0.23 cum Cement Mortar For 1 cum red brick work.

ANALYSIS OF MORTAR REQUIRE FOR 1 CUM AAC WORK		
Volume of 1 AAC (without mortar)	0.6X0.2X0.1	0.012 cum
No. of brick required without mortar	Volume of 1cum brick work/Volume of brick without mortar $1 / 0.012$	83 Nos.
Add 5 mm mortar thickness		
Volume of AAC with mortar	0.605 X 0.205 X 0.105	0.0130 cum
No. of brick required with mortar	Volume of 1cum work/Volume of brick with mortar $1/0.0130$	77 Nos.
Quantity of mortar for 1 cum work		
Quantity of mortar volume	Volume of Brick work – (Volume of AAC Block without mortar x Number of AAC Block required with mortar) $1 - (0.012 \times 77)$	0.076 cum.

(aac-blocks-cement-sand-required)

- There is need of 77 AAC block and 0.076 cum Cement Mortar For 1 cum AAC block work.

3.12 COMPARATIVE ANALYSIS- AAC Blocks vs red Bricks (rate analysis)

ANALYSIS OF CEMENT AND SAND REQUIRE FOR 1 CUM BRICKWORK		
Wet Volume of cement mortar		0.23 cum
Dry volume of mortar	0.23×1.33	0.3059 cum
Mortar Ratio (C:S ratio)		1:4
Cement required		
Cement in cum = (volume of mortar X ratio of cement) / sum of ratio	$0.306 / 5$	0.0612 cum
Cement in kg	0.0612×1440	88.13 kg
Cement in bag	$88.13/50$	1.76 bags.
Sand required		
Sand in cum = (Volume of Mortar x Ratio of sand) / (Sum of Ratio)	$(0.306 \times 4) / (1+4) = 1.224/5$	0.245 cum

ANALYSIS OF CEMENT AND SAND REQUIRE FOR 1 CUM AAC WORK		
Wet Volume of cement mortar		0.076 cum
Dry volume of mortar	0.076×1.33	0.1011 cum
Mortar Ratio (C:S ratio)		1:4
Cement required		
Cement in cum = (volume of mortar X ratio of cement) / sum of ratio	$0.1011 / 5$	0.02022 cum
Cement in kg	0.02022×1440	29.11 kg
Cement in bag	$29.11 / 50$	0.58 bags.
Sand required		
Sand in cum = (Volume of Mortar x Ratio of sand) / (Sum of Ratio)	$(0.1011 \times 4) / (1+4) = 0.4044/5$	0.081 cum

(aac-blocks-cement-sand-required)

3.13 COMPARATIVE ANALYSIS- AAC Blocks vs red Bricks (material rate analysis)

ANALYSIS OF RATE IN 1 CUM BRICK WORK		
Rate of one brick	8.00 Rs	
Rate of Brick used in 1 cum	446×8	3568.00
Rate of one cement bag	350.00 Rs/bag	
Rate of Cement used 1 cum	1.76×350	616.00
Rate of sand (cum)	2150 rs/cum	
Sand	2150×0.245	527.00
(Material Cost)		4711.00 rs
Labour cost		3200.00 rs
Total cost		7911 rs/cum

(rate-analysis-of-brickwork)

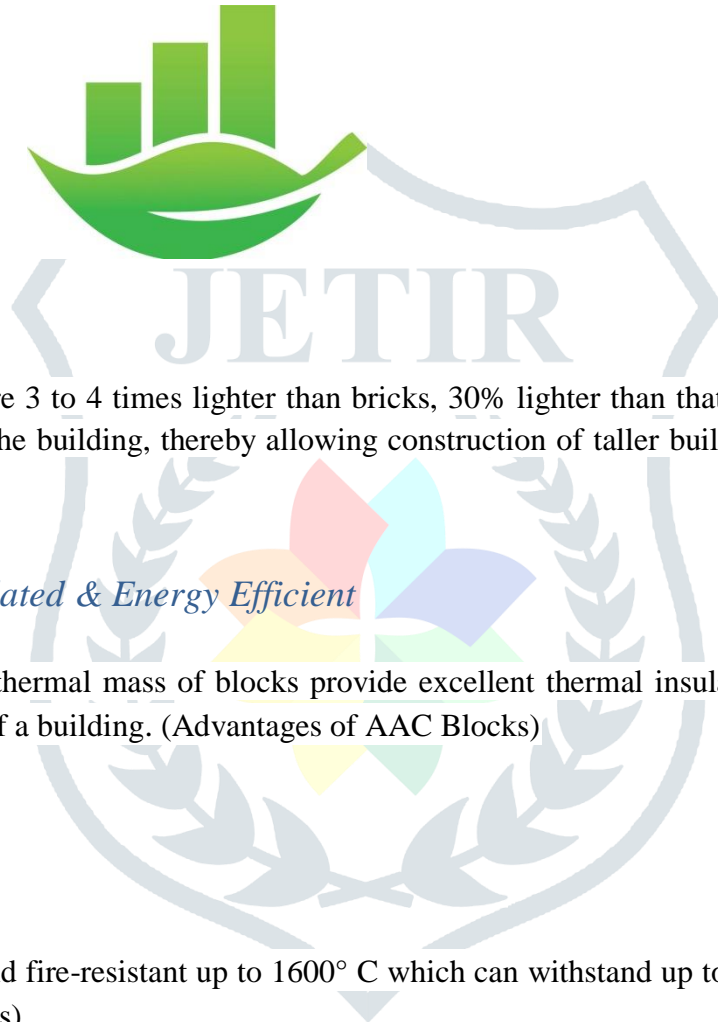
ANALYSIS OF RATE IN 1 CUM BRICK WORK		
Rate of one brick	32.00 Rs	
Rate of Brick used in 1 cum	83×32	
Rate of one cement bag	350.00 Rs/bag	
Rate of Cement used 1 cum	0.58×350	203.00
Rate of sand (cum)	2150 rs/cum	
Sand	2150×0.081	174.15
(Material Cost)		3033.15 rs
Labour cost		2100.00 rs
Total cost		5133 R s/cum

(aac-block-wall)

3.14 Advantages of AAC Blocks

➤ *Eco-Friendly and Sustainable*

The use of recycled industrial waste (fly ash), non-toxic ingredients, no emitting gases, and fewer energy consumptions makes the AAC Blocks eco-friendly and sustainable (Advantages of AAC Blocks)



➤ *Lightweight*

The AAC Blocks are 3 to 4 times lighter than bricks, 30% lighter than that of concrete which helps in reducing the dead load of the building, thereby allowing construction of taller buildings. (Advantages of AAC Blocks)

➤ *Thermally Insulated & Energy Efficient*

Tiny air pores and thermal mass of blocks provide excellent thermal insulation, thus reducing heating and air conditioning costs of a building. (Advantages of AAC Blocks)

➤ *Fire Resistant*

Non-combustible and fire-resistant up to 1600° C which can withstand up to 6 hours of direct exposure. (Advantages of AAC Blocks)



➤ *Acoustic Performance*

As the AAC block is porous in nature, the sound absorption quality is superior. It offers sound attenuation of about 42 dB, blocking out all major sounds and disturbances which makes it ideal for schools, hospitals, hotels, offices, multi-family housing and other structures that require acoustic insulation (Advantages of AAC Blocks)

➤ *Easy Workability and Design Flexibility*

AAC blocks can be easily cut, drilled, nailed, milled and grooved to fit individual requirements. (Advantages of AAC Blocks)

- *Seismic Resistant*

Lightweight blocks reduce the mass of a structure, thus decreasing the impact of an earthquake on a building. Non-combustible nature provides an advantage against fires, which commonly accompany earthquakes. (Advantages of AAC Blocks)

- *Faster Construction*

Construction of AAC Blocks reduces the construction time by 20%. As different sizes of blocks help reduce the number of joints in wall masonry. The lighter weight of the blocks makes it easier and faster to transport, place and construct the masonry. (Advantages of AAC Blocks)

3.15 Environmental Benefits of AAC Blocks

- The AAC blocks or panels have **lower embodied energy** per square meter than a concrete alternative building material.
- The AAC block and panels have **more insulation** value and thus it has low energy usage for heating and cooling loads requirement.
- The total energy used in manufacturing the AAC blocks is around 50% less than that of manufacturing other prefabricated building components and products.
- As compared to regular cement concrete building products, AAC reduces around one-third of the environmental waste.
- The Autoclaved Aerated Concrete (AAC) blocks and panels have proven to be more durable, provide thermal insulation and structural requirements, and also have major economic and environmental benefits as compared to other traditional building components and products.

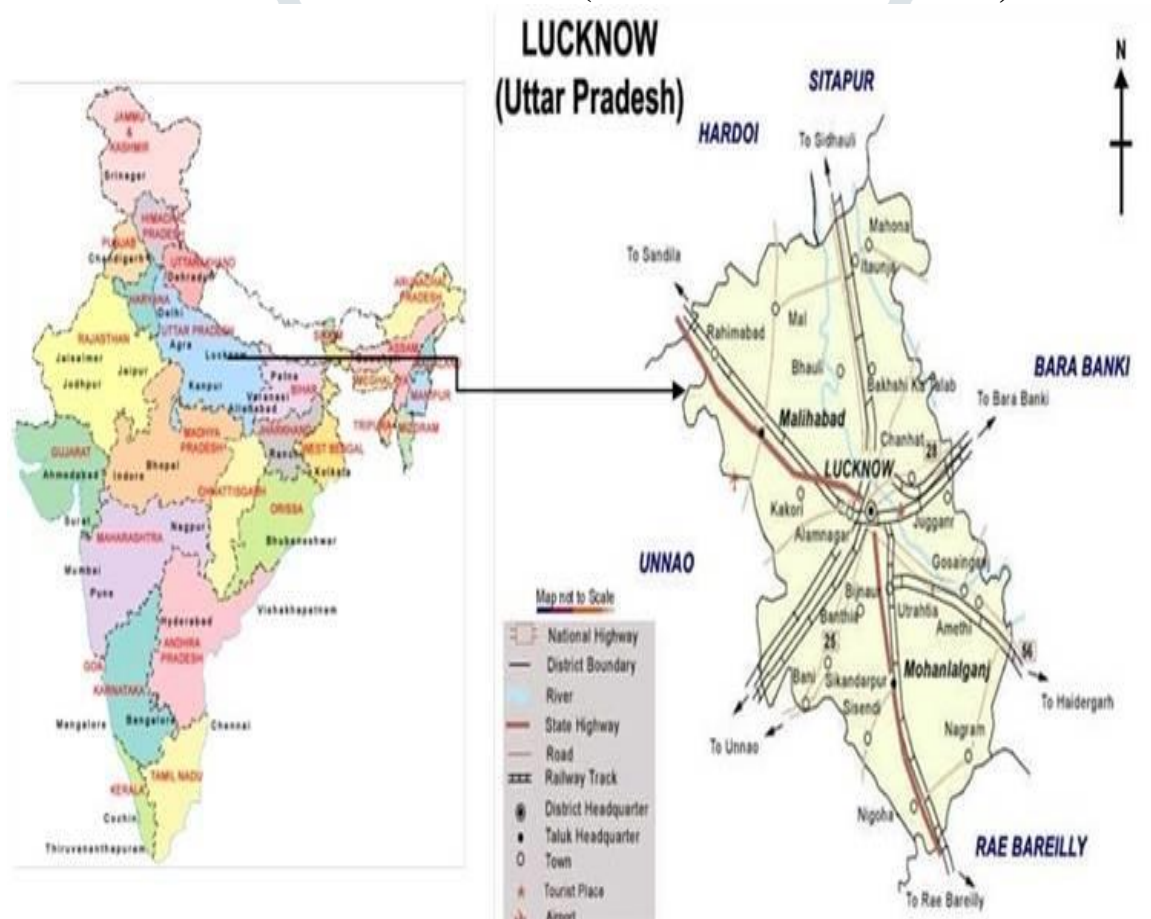
CHAPTER 4

CASE STUDIES

4.1 SELECTION CRITERIA

1. **Building Location:** All case studies are based in Indian context.
2. **Building type:** Residential buildings are taken for case studies.
3. **Number of floors:** Case studies are restricted to mid- rise buildings.
4. **Building Material:** Case studies will be restricted to only those buildings in which the AAC block walls are used.

4.2 SELECTION CASE STUDIES – 01 (VIKAS JI RESIDENCE , LUCKNOW)



Architect: PRASHANT PAL

Year of Construction: 2021

Location: LUCKNOW, UTTAR PRADESH

Climate: COMPOSITE

Building use: Residential

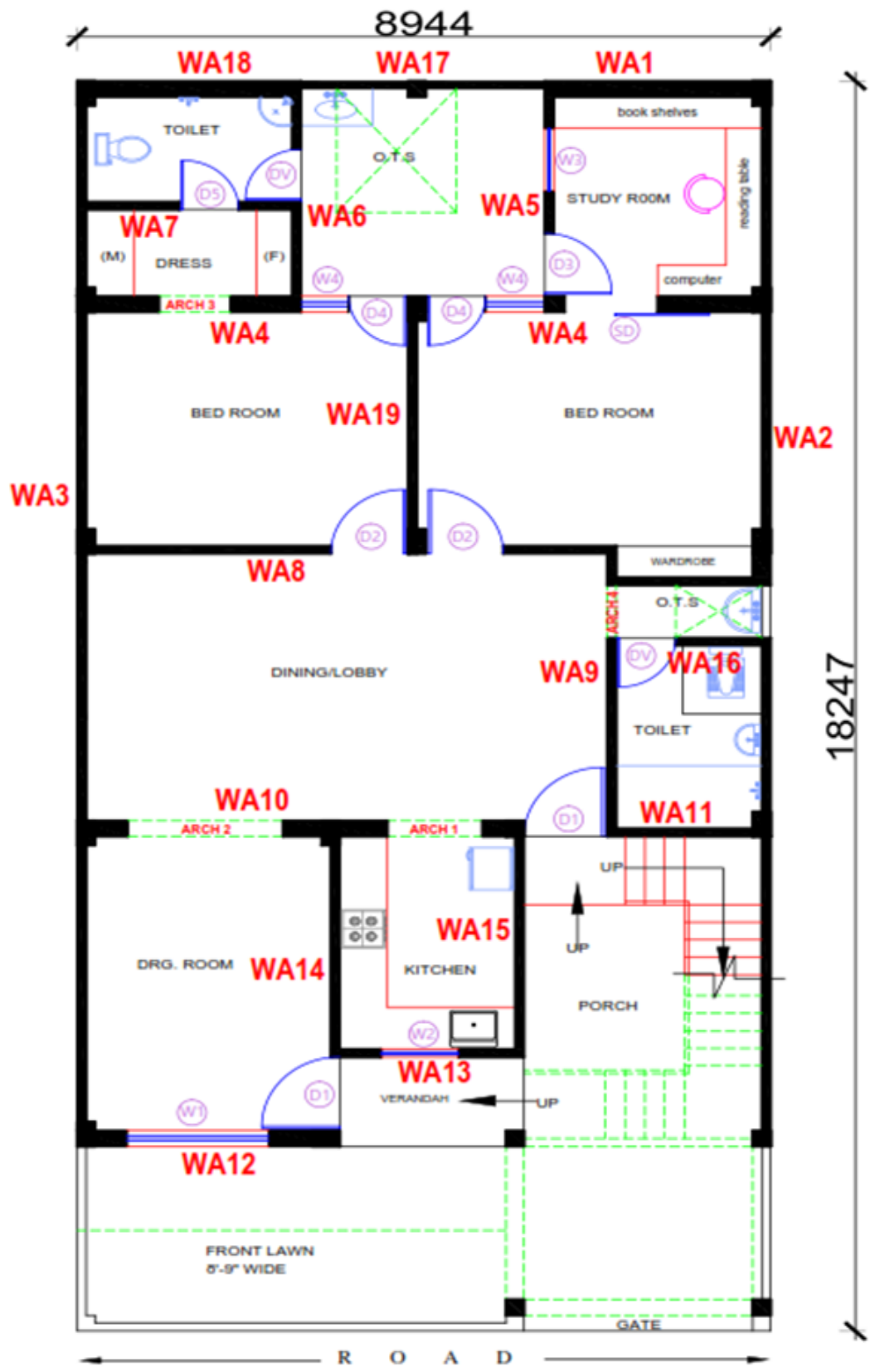
Floors: G+3

Area – 180.00 sq. mt.

4.2.1 PROJECT DESCRIPTION

This building have both commercial and residence use. The basement of building have used for domestic store. The upper ground floor and first floor have space for commercial utilization. The second floor is the residence of the owner.





GROUND FLOOR PLAN

4.2.2 Brick Wall Estimation (ground floor)

S.NO.	WALL TYPE	LENGTH (Mt.)	BREADTH (Mt.)	HEIGHT (Mt.)	VOLUME (CUM.)	
						SAY
1	WA1	2.913	0.230	3.00	2.01	2.10
2	WA2	15.551	0.115	3.00	5.37	5.40
3	WA3	15.551	0.115	3.00	5.37	5.40
4	WA4	8.714	0.230	3.00	6.01	6.10
5	WA5	3.028	0.115	3.00	1.04	1.10
6	WA6	3.028	0.115	3.00	1.04	1.10
7	WA7	2.658	0.115	3.00	0.92	1.00
8	WA8	8.714	0.115	3.00	3.01	3.10
9	WA9	4.012	0.115	3.00	1.38	1.40
10	WA10	5.648	0.115	3.00	1.95	2.00
11	WA11	3.067	0.115	3.00	1.06	1.10
12	WA12	3.271	0.230	3.00	2.26	2.30
13	WA13	2.377	0.115	3.00	0.82	0.90
14	WA14	4.293	0.115	3.00	1.48	1.50
15	WA15	3.105	0.115	3.00	1.07	1.10
16	WA16	1.878	0.115	3.00	0.65	0.70
17	WA17	3.143	0.115	3.00	1.08	1.10
18	WA18	2.888	0.230	3.00	1.99	2.00
19	WA19	3.412	0.115	3.00	1.18	1.20

TOTAL		39.69	39.70
--------------	--	--------------	--------------

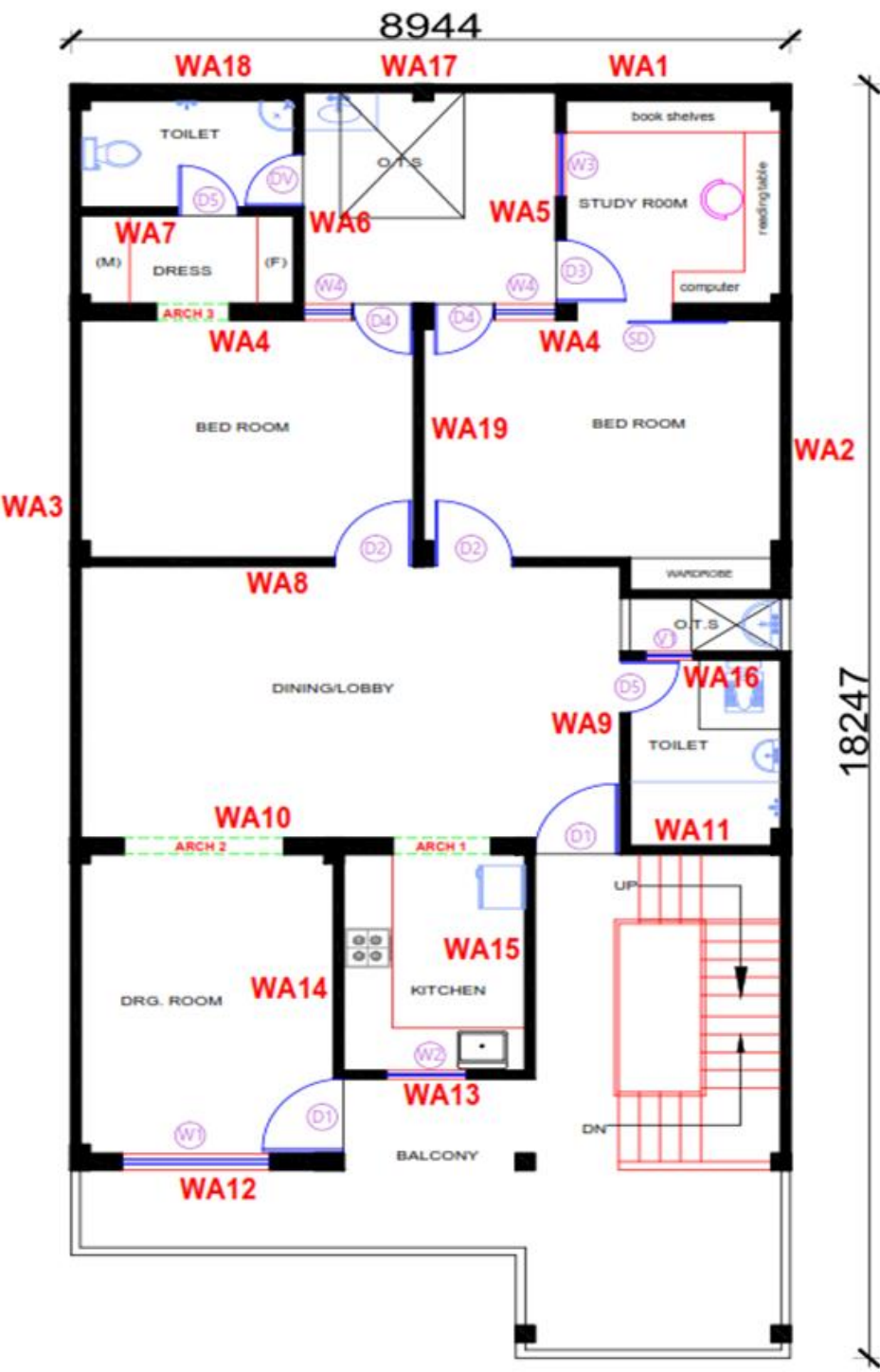
4.2.3 Volume of Door/Window Opening

S.NO.	DOOR / WINDO W TYPE	LENGTH (Mt.)	BREADTH (Mt.)	HEIGHT (Mt.)	VOLUME (CUM.)	NOS.	TOTAL VOLUME (CUM.)	
								SAY
1	D1	1.05	0.115	2.10	0.25	2.0	0.51	0.60
2	D2	1.00	0.115	2.10	0.24	2.0	0.48	0.50
3	D3	0.90	0.115	2.10	0.22	1.0	0.22	0.30
4	D4	0.80	0.23	2.10	0.39	2.0	0.77	0.80
5	D5	0.75	0.115	2.10	0.18	1.0	0.18	0.20
6	DV	0.08	0.115	2.55	0.02	2.0	0.04	0.10
7	SD	1.20	0.23	2.10	0.58	1.0	0.58	0.60
8	W1	1.80	0.23	1.50	0.62	1.0	0.62	0.70
9	W2	1.00	0.115	1.05	0.12	1.0	0.12	0.20
10	W3	0.90	0.115	1.50	0.16	1.0	0.16	0.20
11	W4	0.75	0.23	1.50	0.26	2.0	0.52	0.60
12	ARCH 1	1.20	0.23	2.10	0.58	1.0	0.58	0.60
13	ARCH 2	2.00	0.23	2.10	0.97	1.0	0.97	1.00
14	ARCH 3	0.90	0.115	2.10	0.22	1.0	0.22	0.30
15	ARCH 4	0.76	0.115	2.10	0.18	1.0	0.18	0.20

TOTAL		6.15	6.20
--------------	--	-------------	-------------

Volume of total brick wall construction = total volume - (total volume of windows + total volume of doors)

Volume of total wall construction - 39.70-6.20 = 33.5 cum (G. FLOOR)



FIRST FLOOR PLAN

4.2.4 Brick Wall Estimation (first floor)

S.NO.	WALL TYPE	LENGTH (Mt.)	BREADTH (Mt.)	HEIGHT (Mt.)	VOLUME (CUM.)	
						SAY
1	WA1	2.913	0.230	3.00	2.01	2.10
2	WA2	15.551	0.115	3.00	5.37	5.40
3	WA3	15.551	0.115	3.00	5.37	5.40
4	WA4	8.714	0.230	3.00	6.01	6.10
5	WA5	3.028	0.115	3.00	1.04	1.10
6	WA6	3.028	0.115	3.00	1.04	1.10
7	WA7	2.658	0.115	3.00	0.92	1.00
8	WA8	8.714	0.115	3.00	3.01	3.10
9	WA9	4.012	0.115	3.00	1.38	1.40
10	WA10	5.648	0.115	3.00	1.95	2.00
11	WA11	3.067	0.115	3.00	1.06	1.10
12	WA12	3.271	0.230	3.00	2.26	2.30
13	WA13	2.377	0.115	3.00	0.82	0.90
14	WA14	4.293	0.115	3.00	1.48	1.50
15	WA15	3.105	0.115	3.00	1.07	1.10
16	WA16	1.878	0.115	3.00	0.65	0.70
17	WA17	3.143	0.115	3.00	1.08	1.10
18	WA18	2.888	0.230	3.00	1.99	2.00
19	WA19	3.412	0.115	3.00	1.18	1.20

TOTAL		39.69	39.70
-------	--	-------	-------

4.2.5 Volume of Door/Window Openings

S.NO.	DOOR / WINDO W TYPE	LENGTH (Mt.)	BREADTH (Mt.)	HEIGHT (Mt.)	VOLUME (CUM.)	NOS.	TOTAL VOLUME (CUM.)	
								SAY
1	D1	1.05	0.115	2.10	0.25	2.0	0.51	0.60
2	D2	1.00	0.115	2.10	0.24	2.0	0.48	0.50
3	D3	0.90	0.115	2.10	0.22	1.0	0.22	0.30
4	D4	0.80	0.23	2.10	0.39	2.0	0.77	0.80
5	D5	0.75	0.115	2.10	0.18	2.0	0.36	0.20
6	DV	0.08	0.115	2.55	0.02	1.0	0.02	0.10
7	SD	1.20	0.23	2.10	0.58	1.0	0.58	0.60
8	W1	1.80	0.23	1.50	0.62	1.0	0.62	0.70
9	W2	1.00	0.115	1.05	0.12	1.0	0.12	0.20
10	W3	0.90	0.115	1.50	0.16	1.0	0.16	0.20
11	W4	0.75	0.23	1.50	0.26	2.0	0.52	0.60
12	V1	0.60	0.115	0.45	0.03	1.0	0.03	0.10
13	ARCH 1	1.20	0.23	2.10	0.58	1.0	0.58	0.60
14	ARCH 2	2.00	0.23	2.10	0.97	1.0	0.97	1.00
15	ARCH 3	0.90	0.115	2.10	0.22	1.0	0.22	0.30

TOTAL		6.15	6.20
-------	--	------	------

Volume of total brick wall construction = total volume - (total volume of windows + total volume of doors)

Volume of total wall construction - 39.70-6.20 = 33.5 cum (F. FLOOR)

a) Volume of one red brick = 0.23X0.100 X 0.075

= 0.001725 cum

b) Volume of one AAC block = $0.6 \times 0.2 \times 0.1$

$$= 0.012 \text{ cum}$$

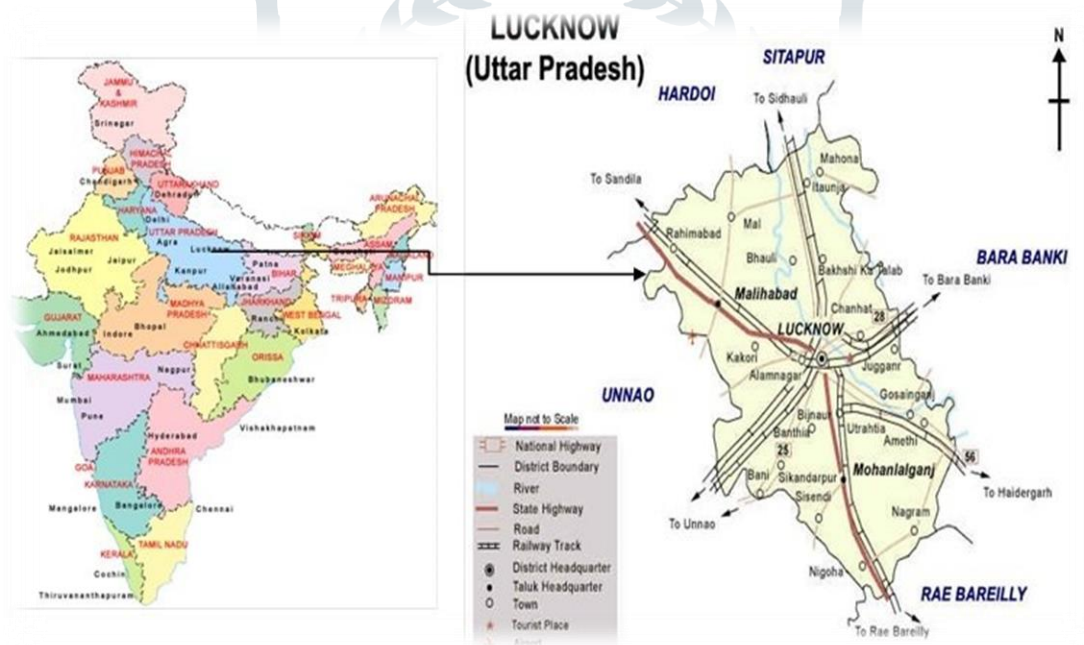
c) Total Volume of wall construction = $33.5 + 33.5 = 67.00 \text{ cum}$

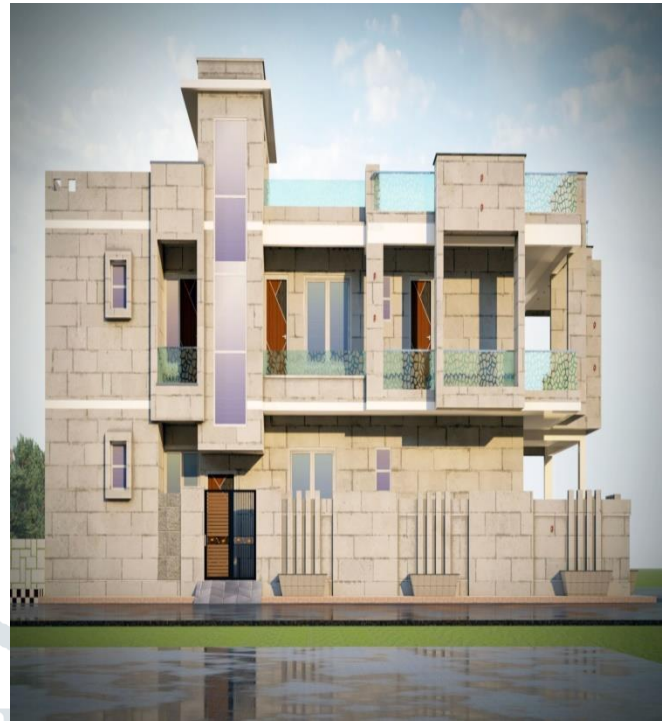
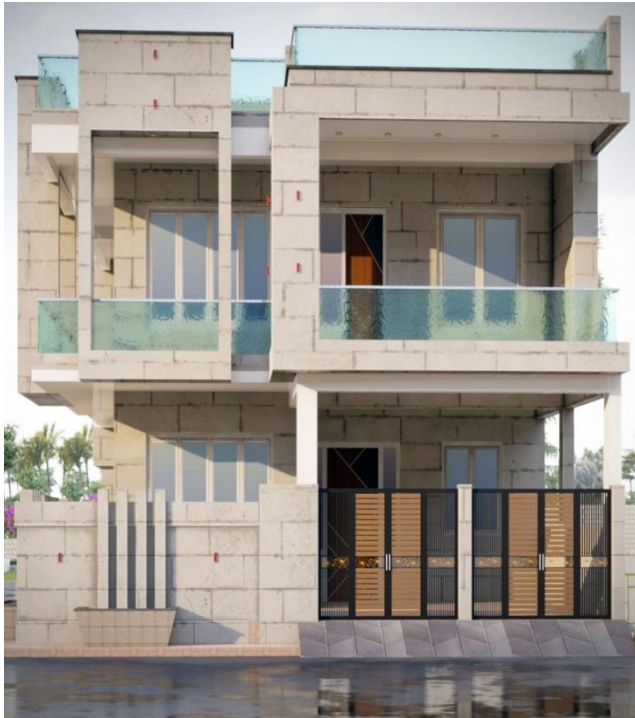
d) No of AAC block used – $67.00 / 0.012 = 5,583.00 \text{ nos.}$

e) No of red bricks used = $67.00 / 0.001725 = 38,840.00 \text{ nos.}$

4.3 CASE STUDIES-02 (RAHBHAR JI RESIDENCE, LUCKNOW)

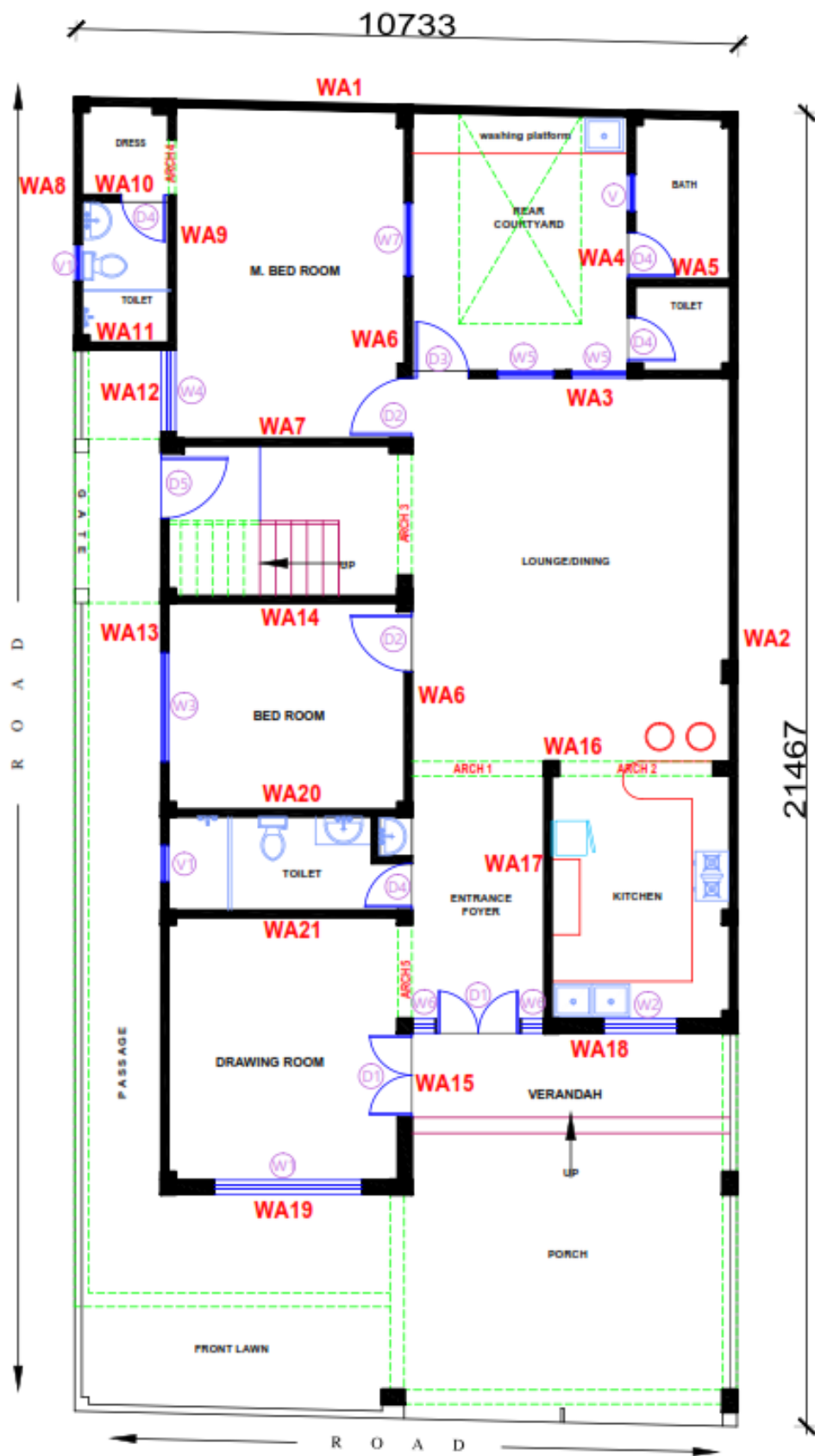
- **Architect:** PRASHANT PAL
- **Year of Construction:** 2021
- **Location:** LUCKNOW, UTTAR PRADESH
- **Climate:** COMPOSITE
- **Building use:** Residential
- **Floors:** G+2
- **Area** – 230.00 sq. mt.





• PROJECT DESCRIPTION

This building have both commercial and residence use. The basement of building have used for domestic store. The upper ground floor and first floor have space for commercial utilization. The second floor is the residence of the owner.



GROUND FLOOR PLAN**Brick Wall Estimation (ground floor)**

S.NO.	WALL TYPE	LENGTH (Mt.)	BREADTH (Mt.)	HEIGHT (Mt.)	VOLUME (CUM.)	
						SAY
1	WA1	10.733	0.115	3.00	3.70	3.70
2	WA2	15.039	0.115	3.00	5.19	5.20
3	WA3	5.149	0.115	3.00	1.78	1.80
4	WA4	4.159	0.115	3.00	1.43	1.50
5	WA5	1.533	0.115	3.00	0.53	0.60
6	WA6	13.043	0.115	3.00	4.50	4.50
7	WA7	3.833	0.115	3.00	1.32	1.40
8	WA8	4.120	0.115	3.00	1.42	1.50
9	WA9	3.971	0.115	3.00	1.37	1.40
10	WA10	1.403	0.115	3.00	0.48	0.50
11	WA11	1.403	0.115	3.00	0.48	0.50
12	WA12	1.458	0.230	3.00	1.01	1.10
13	WA13	12.344	0.115	3.00	4.26	4.30
14	WA14	3.833	0.115	3.00	1.32	1.40
15	WA15	4.638	0.230	3.00	3.20	3.20
16	WA16	5.149	0.230	3.00	3.55	3.60
17	WA17	3.966	0.115	3.00	1.37	1.40
18	WA18	5.149	0.230	3.00	3.55	3.60
19	WA19	3.718	0.230	3.00	2.57	2.60
20	WA20	3.833	0.115	3.00	1.32	1.40
21	WA21	3.833	0.115	3.00	1.32	1.40

TOTAL		45.68	45.70
--------------	--	--------------	--------------

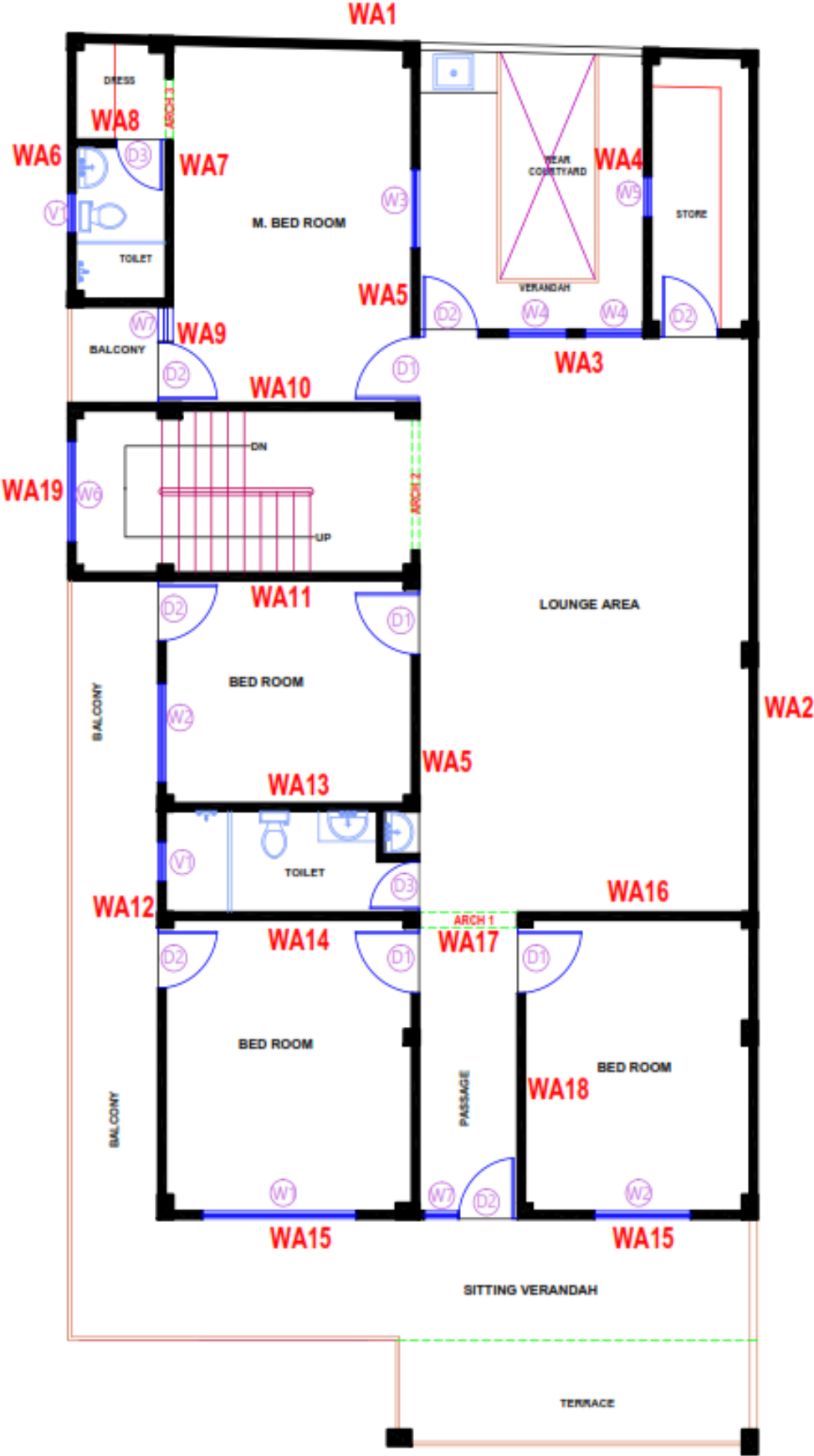
Volume of Door/Window Openings

S.NO.	DOOR / WINDO W TYPE	LENGTH (Mt.)	BREADTH (Mt.)	HEIGHT (Mt.)	VOLUME (CUM.)	NOS.	TOTAL VOLUME (CUM.)	
								SAY
1	D1	1.35	0.23	2.10	0.65	2.0	1.30	1.30
2	D2	1.00	0.115	2.10	0.24	2.0	0.48	0.50
3	D3	0.90	0.115	2.10	0.22	1.0	0.22	0.30
4	D4	0.75	0.115	2.10	0.18	4.0	0.72	0.80
5	D5	1.05	0.115	2.10	0.25	1.0	0.25	0.30
6	W1	2.40	0.23	1.50	0.83	1.0	0.83	0.90
7	W2	1.20	0.23	1.05	0.29	1.0	0.29	0.30
8	W3	1.80	0.115	1.50	0.31	1.0	0.31	0.40
9	W4	1.35	0.23	1.50	0.47	1.0	0.47	0.50
10	W5	0.90	0.115	1.50	0.16	2.0	0.31	0.40
11	W6	0.30	0.23	1.50	0.10	2.0	0.21	0.30
12	W7	1.20	0.115	1.50	0.21	1.0	0.21	0.30
13	V1	0.60	0.115	0.45	0.03	3.0	0.09	0.10
14	ARCH 1	2.10	0.23	2.10	1.01	1.0	1.01	1.10
15	ARCH 2	2.50	0.23	2.10	1.21	1.0	1.21	1.30
16	ARCH 3	2.00	0.23	2.10	0.97	1.0	0.97	1.00
17	ARCH 4	0.90	0.115	2.10	0.22	1.0	0.22	0.30
18	ARCH 5	1.50	0.23	2.10	0.72	1.0	0.72	0.80

TOTAL		9.82	9.90
-------	--	------	------

Volume of total brick wall construction = total volume - (total volume of windows + total volume of doors)

Volume of total wall construction - 45.70-9.90 = 35.8 cum (G. FLOOR)



FIRST FLOOR PLAN**Brick Wall Estimation (first floor)**

S.NO.	WALL TYPE	LENGTH (Mt.)	BREADTH (Mt.)	HEIGHT (Mt.)	VOLUME (CUM.)	
						SAY
1	WA1	10.733	0.115	3.00	3.70	3.70
2	WA2	17.672	0.115	3.00	6.10	5.20
3	WA3	5.149	0.115	3.00	1.78	1.80
4	WA4	4.159	0.115	3.00	1.43	1.50
5	WA5	17.684	0.115	3.00	6.10	0.60
6	WA6	4.120	0.115	3.00	1.42	4.50
7	WA7	4.120	0.115	3.00	1.42	1.40
8	WA8	1.403	0.115	3.00	0.48	1.50
9	WA9	1.458	0.230	3.00	1.01	1.40
10	WA10	5.236	0.115	3.00	1.81	0.50
11	WA11	5.236	0.115	3.00	1.81	0.50
12	WA12	9.660	0.115	3.00	3.33	1.10
13	WA13	3.833	0.115	3.00	1.32	4.30
14	WA14	3.833	0.115	3.00	1.32	1.40
15	WA15	9.328	0.115	3.00	3.22	3.20
16	WA16	3.616	0.115	3.00	1.25	3.60
17	WA17	1.533	0.115	3.00	0.53	1.40
18	WA18	4.408	0.115	3.00	1.52	3.60
19	WA19	2.684	0.115	3.00	0.93	2.60

TOTAL		40.48	45.70
--------------	--	--------------	--------------

Volume of Door/Window Openings

S.NO.	DOOR / WINDOW TYPE	LENGTH (Mt.)	BREADTH (Mt.)	HEIGHT (Mt.)	VOLUME (CUM.)	NOS.	TOTAL VOLUME (CUM.)	
								SAY
1	D1	1.00	0.115	2.10	0.24	4.0	0.97	1.00
2	D2	0.90	0.115	2.10	0.22	6.0	1.30	1.30
3	D3	0.75	0.115	2.10	0.18	2.0	0.36	0.40
4	W1	2.40	0.115	1.50	0.41	1.0	0.41	0.50
5	W2	1.50	0.115	1.50	0.26	2.0	0.52	0.60
6	W3	1.20	0.115	1.50	0.21	1.0	0.21	0.30
7	W4	0.90	0.115	1.50	0.16	2.0	0.31	0.40
8	W5	0.60	0.115	1.50	0.10	1.0	0.10	0.10
9	W6	1.50	0.115	1.20	0.21	1.0	0.21	0.30
10	W7	0.50	0.115	1.50	0.09	2.0	0.17	0.20
11	V1	0.60	0.23	0.45	0.06	2.0	0.12	0.20
12	ARCH 1	1.50	0.115	2.10	0.36	1.0	0.36	0.40
13	ARCH 2	2.00	0.115	2.10	0.48	1.0	0.48	0.50
14	ARCH 3	0.90	0.115	2.10	0.22	1.0	0.22	0.30

TOTAL		5.75	5.80
--------------	--	-------------	-------------

Volume of total brick wall construction = total volume - (total volume of windows + total volume of doors)

Volume of total wall construction - 45.70-5.80 = 39.9 cum (F. FLOOR)

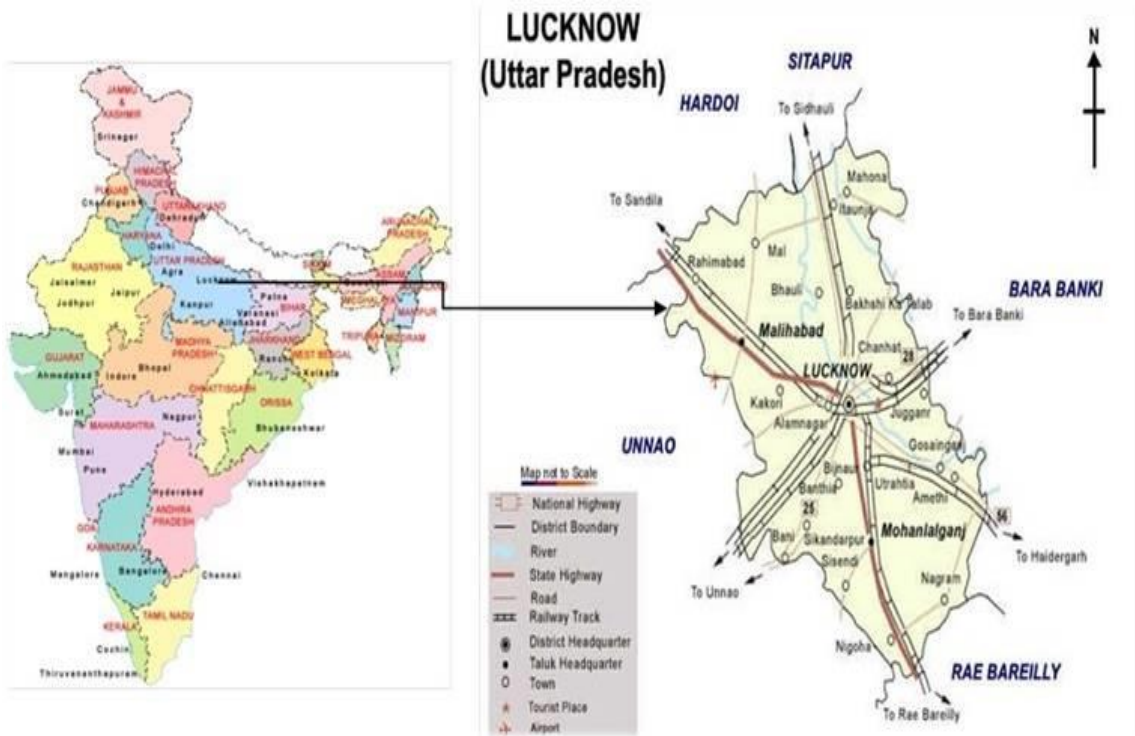
- a) Volume of one AAC block = $0.6 \times 0.2 \times 0.1$
= 0.012 cum
- b) Volume of one red brick = $0.23 \times 0.100 \times 0.075$
= 0.001725 cum
- c) Total Volume of wall construction = $35.8 + 39.9 = 75.70$ cum
- d) No of red bricks used = $75.70 / 0.001725 = 43,884.00$ nos.
- e) No of AAC block used = $75.70 / 0.012 = 6,308.00$ nos.

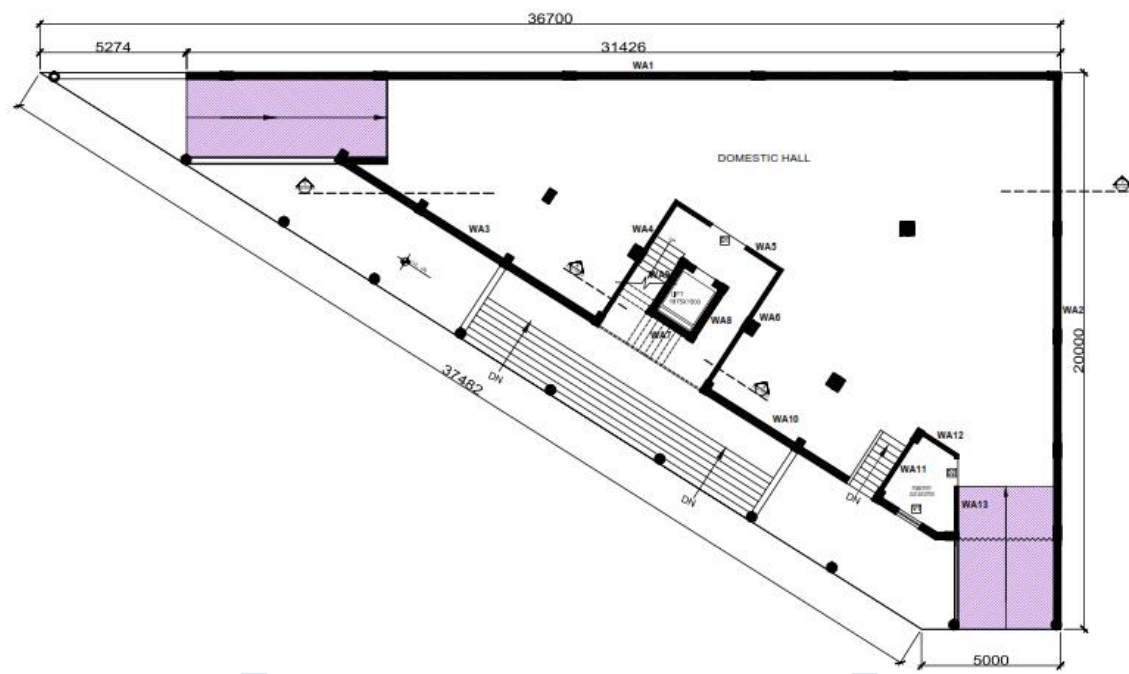
- **CASE STUDIES-03 (K K PALACE , LUCKNOW)**

- *Architect: Sanjoli Pal*
- *Year of Construction: 2018*
- *Location: LUCKNOW, UTTAR PRADESH*
- *Climate: COMPOSITE*
- *Building use: Residential*
- *Floors: G+3*
- *Area – 412.sq mt.*

- **PROJECT DESCRIPTION**

This building have both commercial and residence use. The basement of building have used for domestic store. The upper ground floor and first floor have space for commercial utilization. The second floor is the residence of the owner.





BASEMENT FLOOR PLAN

Brick Wall Estimation (basement floor)

S.NO.	WALL TYPE	LENGTH (Mt.)	BREADTH (Mt.)	HEIGHT (Mt.)	VOLUME (CUM.)	
						SAY
1	WA1	31.426	0.23	2.70	19.52	19.60
2	WA2	20.0	0.23	2.70	12.42	12.50
3	WA3	10.925	0.23	2.70	6.78	6.80
4	WA4	4.981	0.115	2.70	1.55	1.60
5	WA5	4.597	0.115	2.70	1.43	1.50
6	WA6	4.981	0.115	2.70	1.55	1.60
7	WA7	1.96	0.23	2.70	1.22	1.30
8	WA8	2.105	0.23	2.70	1.31	1.40
9	WA9	2.105	0.23	2.70	1.31	1.40
10	WA10	9.991	0.23	2.70	6.20	6.20
11	WA11	2.915	0.115	2.70	0.91	1.00
12	WA12	1.583	0.115	2.70	0.49	0.50
13	WA13	3.045	0.23	2.70	1.89	1.90

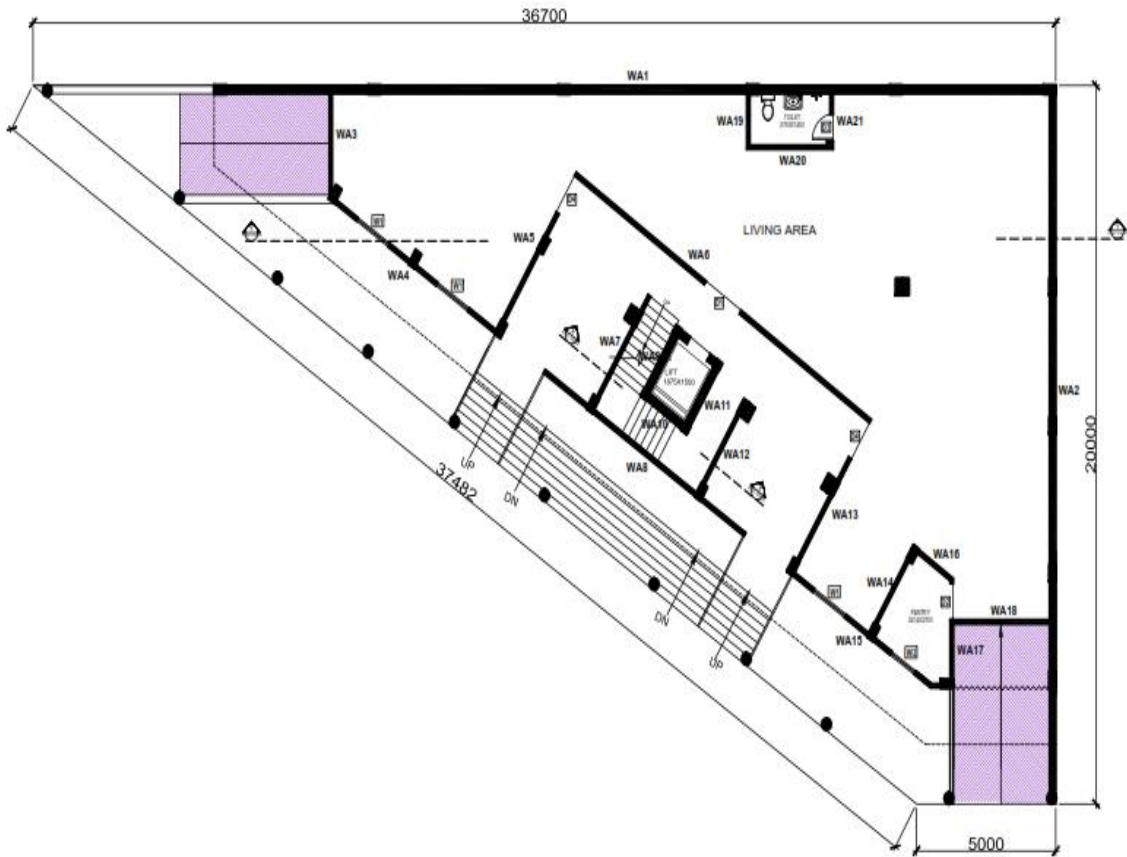
TOTAL		56.56	56.60
-------	--	-------	-------

Volume of Door/Window Openings

S.NO.	DOOR / WINDOW TYPE	LENGTH (Mt.)	BREADTH (Mt.)	HEIGHT (Mt.)	VOLUME (CUM.)	
						SAY
1	D1	1.5	0.115	2.10	0.36	0.40
2	D2	1.0	0.115	2.10	0.24	0.30
3	V1	1.0	0.23	0.45	0.10	0.10

TOTAL		0.71	0.80
-------	--	------	------

- BASEMENT FLOOR PLAN
- Volume of wall construction = 55.88 CUM



GROUND FLOOR PLAN

Brick Wall Estimation (ground floor)

S.NO.	WALL TYPE	LENGTH (Mt.)	BREADTH (Mt.)	HEIGHT (Mt.)	VOLUME (CUM.)	
						SAY
1	WA1	30.201	0.23	3.00	20.84	20.90
2	WA2	20.0	0.23	3.00	13.80	13.90
3	WA3	2.927	0.115	3.00	1.01	1.10
4	WA4	6.802	0.115	3.00	2.35	2.40
5	WA5	5.358	0.115	3.00	1.85	1.90
6	WA6	12.397	0.115	3.00	4.28	4.30
7	WA7	3.738	0.115	3.00	1.29	1.30
8	WA8	8.477	0.115	3.00	2.92	3.00
9	WA9	2.105	0.23	3.00	1.45	1.50
10	WA10	1.96	0.23	3.00	1.35	1.40
11	WA11	2.105	0.23	3.00	1.45	1.50
12	WA12	3.11	0.115	3.00	1.07	1.10
13	WA13	5.358	0.115	3.00	1.85	1.90
14	WA14	2.918	0.115	3.00	1.01	1.10
15	WA15	6.085	0.115	3.00	2.10	2.10
16	WA16	1.583	0.115	3.00	0.55	0.60
17	WA17	3.045	0.115	3.00	1.05	1.10
18	WA18	3.453	0.115	3.00	1.19	1.20
19	WA19	1.78	0.115	3.00	0.61	0.70
20	WA20	2.874	0.115	3.00	0.99	1.00
21	WA21	1.78	0.115	3.00	0.61	0.70

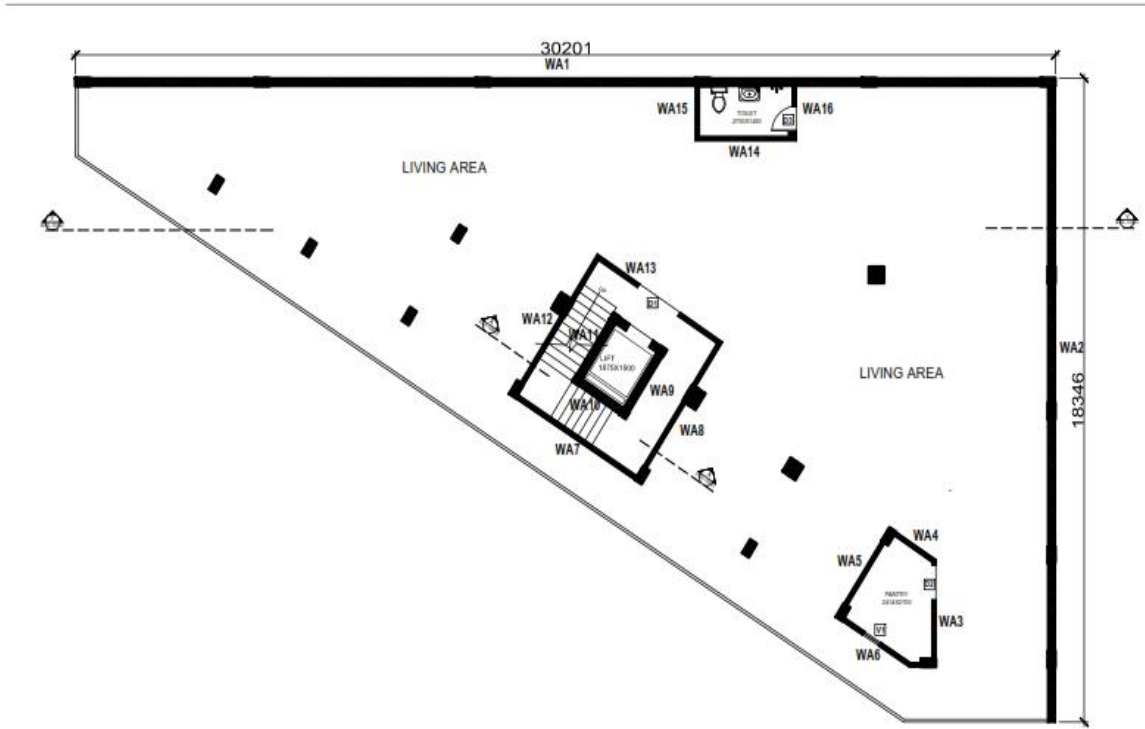
TOTAL		63.63	63.70
-------	--	-------	-------

Volume of Door/Window Openings

S.NO.	DOOR /WINDOW TYPE	LENGTH (Mt.)	BREADT H (Mt.)	HEIGHT (Mt.)	VOLUME (CUM.)	NOS.	TOTAL VOLUME (CUM.)	
								SAY
1	D1	1.5	0.115	2.10	0.36	1.00	0.36	0.40
2	D2	1.0	0.115	2.10	0.24	1.00	0.24	0.30
3	D3	0.75	0.115	2.10	0.18	1.00	0.18	0.20
4	D4	1.2	0.115	2.10	0.29	2.00	0.58	0.60
5	W1	1.35	0.115	0.45	0.07	3.00	0.21	0.30
6	W2	1.0	0.115	0.45	0.05	1.00	0.05	0.10

TOTAL		1.63	1.70
-------	--	------	------

- GROUND FLOOR PLAN
- Volume of wall construction = 62.00 CUM



FIRST FLOOR PLAN

Volume of Door/Window Openings

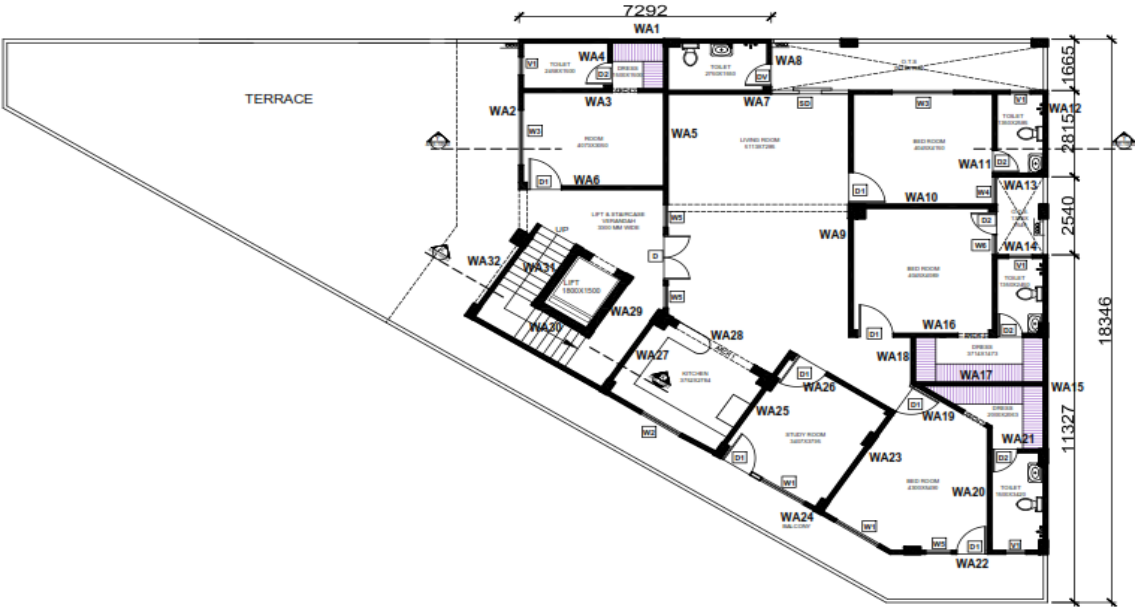
S.NO.	DOOR / WINDOW TYPE	LENGTH (Mt.)	BREADTH (Mt.)	HEIGHT (Mt.)	VOLUME (CUM.)	
						SAY
1	D1	1.5	0.115	2.10	0.36	0.40
2	D2	1.0	0.115	2.10	0.24	0.30
3	D3	0.75	0.115	2.10	0.18	0.20
4	V1	0.6	0.115	0.45	0.03	0.10
TOTAL					0.82	0.90

Brick Wall Estimation (first floor)

S.NO.	WALL TYPE	LENGTH (Mt.)	BREADTH (Mt.)	HEIGHT (Mt.)	VOLUME (CUM.)	
						SAY
1	WA1	30.201	0.23	3.00	20.84	20.90
2	WA2	18.346	0.23	3.00	12.66	12.70
3	WA3	3.045	0.115	3.00	1.05	1.10
4	WA4	1.583	0.115	3.00	0.55	0.60
5	WA5	2.918	0.115	3.00	1.01	1.10
6	WA6	2.561	0.115	3.00	0.88	0.90
7	WA7	4.59	0.115	3.00	1.58	1.60
8	WA8	4.517	0.115	3.00	1.56	1.60
9	WA9	2.105	0.23	3.00	1.45	1.50
10	WA10	1.96	0.23	3.00	1.35	1.40
11	WA11	2.105	0.23	3.00	1.45	1.50
12	WA12	4.517	0.115	3.00	1.56	1.60
13	WA13	4.59	0.115	3.00	1.58	1.60
14	WA14	3.104	0.115	3.00	1.07	1.10
15	WA15	1.435	0.115	3.00	0.50	0.60
16	WA16	1.435	0.115	3.00	0.50	0.50

TOTAL		49.59	49.60
-------	--	-------	-------

- FIRST FLOOR PLAN
- Volume of wall construction = 48.70 CUM



SECOND FLOOR PLAN**Brick Wall Estimation (second floor)**

S.NO.	WALL TYPE	LENGTH (Mt.)	BREADTH (Mt.)	HEIGHT (Mt.)	VOLUME (CUM.)	
						SAY
1	WA1	7.292	0.115	3.00	2.52	2.60
2	WA2	4.780	0.115	3.00	1.65	1.70
3	WA3	4.073	0.115	3.00	1.41	1.50
4	WA4	1.615	0.115	3.00	0.56	0.60
5	WA5	8.869	0.115	3.00	3.06	3.10
6	WA6	4.073	0.115	3.00	1.41	1.50
7	WA7	10.977	0.115	3.00	3.79	3.80
8	WA8	1.55	0.115	3.00	0.53	0.60
9	WA9	7.919	0.115	3.00	2.73	2.80
10	WA10	4.045	0.115	3.00	1.40	1.50
11	WA11	7.804	0.115	3.00	2.69	1.70
12	WA12	2.7	0.115	3.00	0.93	1.00
13	WA13	1.35	0.115	3.00	0.47	0.50
14	WA14	1.35	0.115	3.00	0.47	0.50
15	WA15	9.752	0.115	3.00	3.36	3.40
16	WA16	5.51	0.115	3.00	1.90	1.90
17	WA17	3.714	0.115	3.00	1.28	1.30
18	WA18	1.525	0.115	3.00	0.53	0.60
19	WA19	2.641	0.115	3.00	0.91	1.00
20	WA20	3.993	0.115	3.00	1.38	1.40
21	WA21	1.5	0.115	3.00	0.52	0.60
22	WA22	4.442	0.115	3.00	1.53	1.60
23	WA23	4.869	0.115	3.00	1.68	1.70
24	WA24	14.415	0.115	3.00	4.97	5.00
25	WA25	3.919	0.115	3.00	1.35	1.40
26	WA26	3.407	0.115	3.00	1.18	1.20
27	WA27	2.899	0.115	3.00	1.00	1.00
28	WA28	2.899	0.23	3.00	2.00	2.00
29	WA29	2.105	0.23	3.00	1.45	1.50
30	WA30	1.96	0.23	3.00	1.35	1.40
31	WA31	2.105	0.23	3.00	1.45	1.50
32	WA32	3.523	0.115	3.00	1.22	1.30

TOTAL		52.66	52.70
--------------	--	--------------	--------------

Volume of Door/Window Openings

S.NO.	DOOR / WINDOW TYPE	LENGTH (Mt.)	BREADTH (Mt.)	HEIGHT (Mt.)	VOLUME (CUM.)	NOS.	TOTAL VOLUME (CUM.)	
								SAY
1	DD1	2.2	0.115	2.10	0.53	1.00	0.53	0.60
2	D	1.5	0.115	2.10	0.36	1.00	0.36	0.40
3	D1	1.0	0.115	2.10	0.24	7.00	1.69	1.70
4	D2	0.75	0.115	2.10	0.18	5.00	0.91	1.00
5	D3	0.75	0.115	2.55	0.22	1.00	0.22	0.30
6	W1	1.50	0.115	1.50	0.26	2.00	0.52	0.60
7	W2	1.35	0.115	1.05	0.16	1.00	0.16	0.20
8	W3	1.80	0.115	1.50	0.31	2.00	0.62	0.70
9	W4	0.90	0.115	1.50	0.16	1.00	0.16	0.20
10	W5	0.75	0.115	1.50	0.13	3.00	0.39	0.40
11	W6	0.65	0.115	1.50	0.11	1.00	0.11	0.20
12	ARCH 1	2.59	0.23	2.10	1.25	1.00	1.25	1.30
13	ARCH 2	0.75	0.115	2.10	0.18	3.00	0.54	0.60

TOTAL		7.46	7.50
-------	--	------	------

- SECOND FLOOR PLAN
- Volume of wall construction = 45.20 CUM

a) TOTAL Volume of wall construction (all floors)
= 55.88+ 62.00+48.70+45.20 =211.78 CUM

b) Volume of one red brick = 0.23X0.100 X 0.075
= 0.001725 cum

c) Volume of one AAC brick = 0.6 x 0.2 x 0.1 = 0.012 cum

d) No of red bricks used = 211.78/ 0.001725
= 122771 nos.

e) No of AAC block used = 211.78/ 0.012
= 17648 nos.

Comparative Analysis of Literature studies

S. NO.	PARAMETERS	VIKAS RESIDENCE AAC BLOCK	VIKAS RESIDENCE RED BRICK	RAHBHAR RESIDENCE AAC BLOCK	RAHBHAR RESIDENCE RED BRICK	K K PALACE AAC BLOCK	K K PALACE RED BRICK
1.	NO of Bricks	5583	38840	6308	43884	17648	122771
2.	Volume	67.00 CUM		75.70 CUM		211.78 CUM	
3.	Weight	44664.00 kg	116520.00 kg	50464.00 kg	131652.00 kg	141184.00 kg	368313.00 kg
4.	joints	4150	140700	46934	158970	131304	444738
5.	Cement bags	39 (1950 kg)	118 (5900 kg)	44 (2200 kg)	133 (6650 kg)	123 (6150 kg)	373 (18650 kg)
6.	Cost	3,43,911.00 rs	5,30,037.00 rs	3,88,568.00 rs	5,98,863.00 rs	10,87,067.00 rs	1675392 rs
7.	Carbon emission	15,745.00 kg co2	1,27,300.00 kg co2	17,790.00 kg co2	1,43,830.00 kg co2	49768.00 kg co2	4,02,382 kg co2
8.	Curing time		7 days		7 days		7 days
9.							
10.							

INFERANCES

- Autoclaved aerated concrete (AAC) block masonry has been widely used for bearing walls of multi-story buildings or non-bearing walls of high-rise buildings because of its unique advantages, such as lightweight, low pollution output, and excellent thermal insulation performance.
- Autoclaved Aerated Concrete Block (AAC) are used for load bearing walls proving
- it can be used in multi-storied construction.
- It uses the less mortar and has less joints in wall construction.
- It provides good thermal insulation than conventional brick.
- Use of AAC blocks in construction result in less carbon footprint.



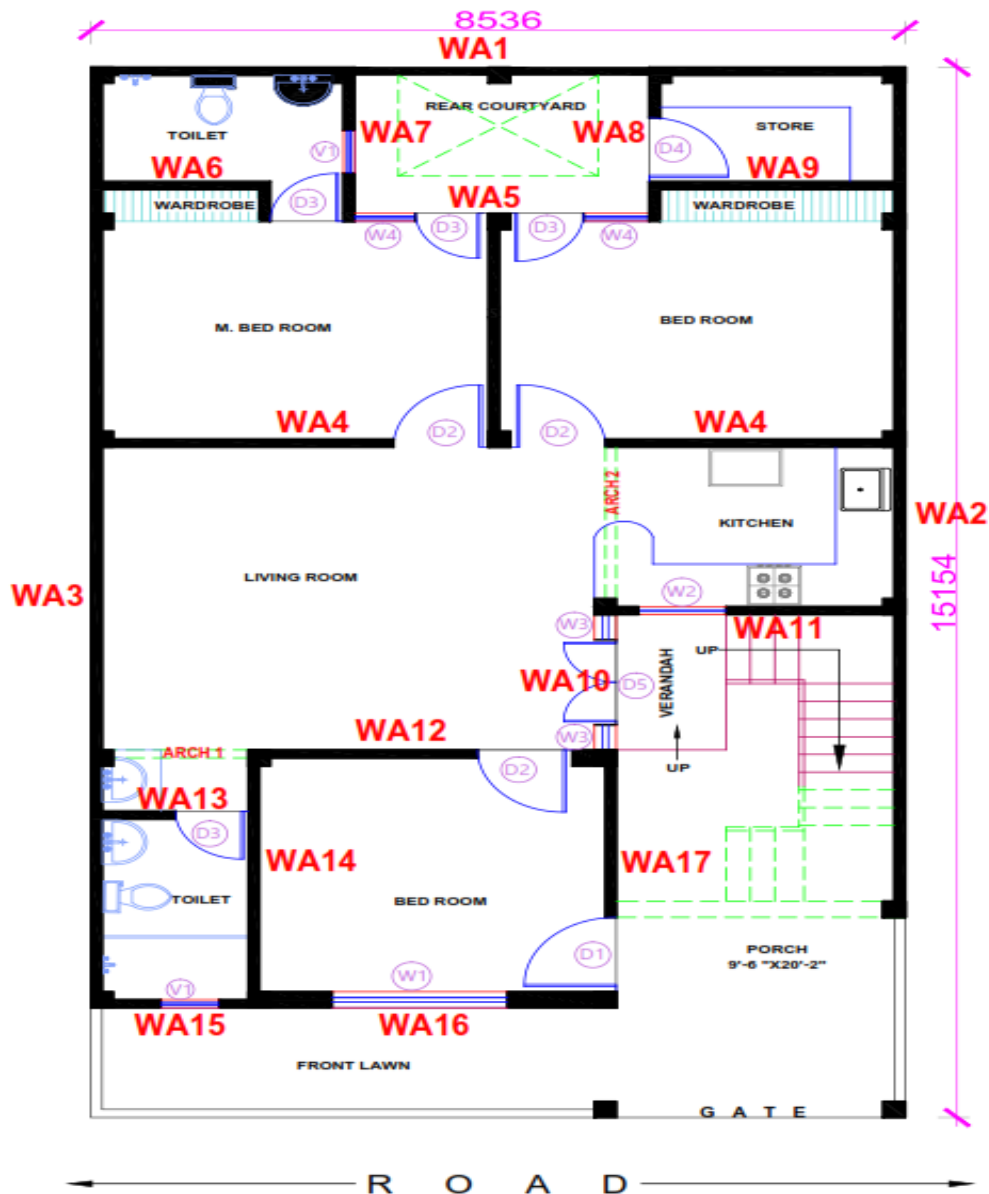
CHAPTER 4

CASE DEVELOPMENT

INTRODUCTION

In order to understand the applicability of AAC blocks as compared to other conventional materials, the development of a case has been done

Lucknow has been chosen as the proposed location for case development so as to take AAC block to site.



GROUND FLOOR

Location: Lucknow, INDIA

Climate: Composite

Building Type: Residence

Floors: Ground floor

Net floor area: 127.5 sq.mt

- Estimation**

AAC Wall Volume Estimation (ground floor)

S.NO.	WALL TYPE	LENGTH (Mt.)	BREADTH (Mt.)	HEIGHT (Mt.)	VOLUME (CUM.)	
						SAY
1	WA1	8.536	0.115	3.00	2.94	3.00
2	WA2	12.152	0.115	3.00	4.19	4.20
3	WA3	13.570	0.115	3.00	4.68	4.70
4	WA4	8.306	0.115	3.00	2.87	2.90
5	WA5	4.654	0.115	3.00	1.61	1.70
6	WA6	1.763	0.115	3.00	0.61	0.70
7	WA7	1.993	0.115	3.00	0.69	0.70
8	WA8	1.993	0.115	3.00	0.69	0.70
9	WA9	2.453	0.115	3.00	0.85	0.90
10	WA10	1.955	0.23	3.00	1.35	1.40
11	WA11	2.913	0.115	3.00	1.00	1.00
12	WA12	3.629	0.115	3.00	1.25	1.30
13	WA13	1.533	0.115	3.00	0.53	0.60
14	WA14	3.488	0.115	3.00	1.20	1.20
15	WA15	1.648	0.115	3.00	0.57	0.60
16	WA16	3.859	0.23	3.00	2.66	2.70
17	WA17	3.718	0.115	3.00	1.28	1.30
			TOTAL		28.97	29.00

Volume of Door/Window Openings

S.NO.	DOOR / WINDO W TYPE	LENGTH (Mt.)	BREADTH (Mt.)	HEIGHT (Mt.)	VOLUME (CUM.)	NOS.	TOTAL VOLUME (CUM.)	
								SAY
1	D1	1.050	0.115	2.10	0.25	1.0	0.25	0.30
2	D2	1.000	0.115	2.10	0.24	2.0	0.48	0.50
3	D3	0.750	0.115	2.10	0.18	4.0	0.72	0.80
4	D4	0.900	0.115	2.10	0.22	1.0	0.22	0.30
5	D5	1.200	0.115	2.55	0.35	1.0	0.35	0.40
6	W1	1.800	0.23	1.50	0.62	1.0	0.62	0.70
7	W2	0.900	0.115	1.05	0.11	1.0	0.11	0.20
8	W3	0.350	0.23	1.50	0.12	2.0	0.24	0.30
9	W4	0.650	0.115	1.50	0.11	2.0	0.22	0.30
10	V1	0.600	0.115	0.45	0.03	2.0	0.06	0.10
11	ARCH 1	1.533	0.115	2.10	0.37	1.0	0.37	0.40
12	ARCH 2	2.300	0.115	2.10	0.56	1.0	0.56	0.60
					TOTAL		4.21	4.30

Volume of total brick wall construction = total volume - (total volume of windows + total volume of doors)

b) Volume of total wall construction = $29.00 - 4.30 = 24.7$ cum (G. FLOOR)

c) Total Volume of wall construction = 24.7 cum

d) Volume of one AAC block = $0.6 \times 0.2 \times 0.1 = 0.012 \text{ cum}$

e) Volume of one red brick = $0.23 \times 0.100 \times 0.075 = 0.001725 \text{ cum}$

f) No AAC block used = $24.7 / 0.012 = 2058.00$ nos.

g) No red bricks used = $75.70 / 0.001725 = 14319.00$ nos

Comparative Analysis of AAC block and conventional brick based on estimation

S.NO.	PARAMETERS	AAC BLOCK	RED BRICK
1.	Size	0.6X.2X0.1	0.230X0.115X0.075
2.	NO of Bricks required	2058	14319
3.	Volume	24.7 CUM	
4.	Weight	16864.00 kg	42957.00 kg
5.	Cement bags	15 (750 kg)	44 (2200 kg)
6.	Cost effectiveness	1,26,785.00 rs Less mortar used due less joints 5% waste generated on site	195401.00 rs Mortar required 10% waste minimum
7.	Carbon emission	AAC produces 130 kg/m ³ For total construction = 3211 kg of CO ₂ /m ³	642.87 Kg of co ₂ For total construction - 15878.8 kg of CO ₂ /m ³
8.	Initial embodied energy (MJ/m ³ of material)	AAC produces 2205.00 MJ/m ³ For total construction – 54463.5 MJ/m ³	6122.54 MJ/m ³ For total construction – 151226.73 MJ/m ³

Conclusion & Recommendation*Conclusions*

- From the case development carried out in this study, the following conclusions can be made concerning the effects of using AAC blocks compared to other conventional materials in construction industry.
- Initial embodied energy of red brick is 151226.73 mj/m³. Autoclaved aerated concrete blocks (AAC) initial embodied energy is 26319.36mj/m³ which is very less compared to kiln red bricks.
- Carbon emission by red brick is 15778.8 kg of CO₂/m³ and Autoclaved aerated concrete blocks (AAC) has 2205.00 kg of CO₂ /m³ very less compared to kiln red bricks and cement blocks.
- AAC block requires less labour and water than the conventional brick in construction.
- Total costing for the Autoclaved aerated concrete blocks (AAC) blocks is Rs. 1,26,785.00 while for red bricks is Rs. 195401.00 proving that if AAC blocks is used and cost 10% - 15% less than other conventional materials.

Recommendation

Based on the above analysis and conclusion, it is seen that the AAC blocks plays a significant role towards sustainable construction. As firewood is not needed to produce AAC, its initial embodied energy as well as carbon emission is way less than other conventional materials.

BIBLIOGRAPHY

aac-blocks-cement-sand-required. (n.d.). Retrieved from <https://civilsuccessonline.com/aac-blocks-cement-sand-required-for-block-work/#:~:text=AAC%20Blocks%2C%20Cement%2C%20Sand%20Required%20For%20Block%20Work&text=The%20block%20wall%20has%20a,240%20mm%20x%20150%20mm./>

aac-blocks-cement-sand-required. (n.d.). Retrieved from <https://civilsuccessonline.com/aac-blocks-cement-sand-required-for-block-work/#:~:text=AAC%20Blocks%2C%20Cement%2C%20Sand%20Required%20For%20Block%20Work&text=The%20block%20wall%20has%20a,240%20mm%20x%20150%20mm./>

aac-blocks-vs-red-bricks-comparison. (n.d.). Retrieved from <https://vincivilworld.com/2020/09/16/aac-blocks-vs-red-bricks-comparison>

aac-blocks-vs-red-bricks-comparison. (n.d.). Retrieved from <https://vincivilworld.com/2020/09/16/aac-blocks-vs-red-bricks-comparison>

aac-blocks-vs-red-bricks-comparison. (n.d.). Retrieved from <https://vincivilworld.com/2020/09/16/aac-blocks-vs-red-bricks-comparison>

aac-block-wall. (n.d.). Retrieved from <https://www.paramvisions.com/2021/06/what-will-be-cost-of-aac-block-wall.html>

Advantages of AAC Blocks. (n.d.). Retrieved from <https://theconstructor.org/building/autoclaved-aerated-cement-blocks-aac-properties-advantages/37211/>

Jayasinghe, C. &. (2009)). *Flexural strength of compressed stabilized earth masonry materials. Materials and Design, 30(9), 3859–3868.* Retrieved from : <https://doi.org/10.1016/j.matdes.2009.01.029>

Raj, A. (2020). Literature Survey and Detailed Objectives. *STRENGTH ENHANCEMENT OF AUTOCLAVED AERATED*, 14-33.

rate-analysis-of-brickwork. (n.d.). Retrieved from <https://wecivilengineers.wordpress.com/2018/03/28/rate-analysis-of-brickwork/>

Vengalais, D. J., ShivakumarMangloor, & Talla Krishna Chaitanya Goud. (2009). *Performance of Autoclaved Aerated Concrete.* Blue Eyes Intelligence Engineering & Sciences Publication.

Wahane, A. (2017). *MANUFACTURING PROCESS OF AAC BLOCK.* Raipur INDIA: International Journal of Advance Research in Science and Engineering.